
Ancient TL

www.ancienttl.org · ISSN: 2693-0935

Issue 39(1) - June 2021

<https://doi.org/10.26034/la.atl.v39.i1>

This issue is published under a Creative Commons Attribution 4.0 International (CC BY):

<https://creativecommons.org/licenses/by/4.0>



© Ancient TL, 2021

Ancient TL

A periodical devoted to Luminescence and ESR dating

Department of Physics, East Carolina University, 1000 East 5th Street, Greenville, NC 27858, USA
<http://ancienttl.org>

June 2021, Volume 39 No.1

| | |
|---------------------------------------------------------------------------------------------------------------|----|
| Safelight for OSL dating laboratories: a follow-up study | 1 |
| Reza Sohbaty, MyungHo Kook, Lars P. Pirtzel, Kristina J. Thomsen | |
| Methods Note: Can hydrogen peroxide digestion of organic matter ever be too aggressive for OSL dating? | 6 |
| Kenneth Lepper, Jenna Fischer | |
| Thesis abstracts | 10 |
| Bibliography | 16 |
| Announcements | 31 |

Ancient TL

Started by the late David Zimmerman in 1977

EDITOR

Regina DeWitt, Department of Physics, East Carolina University, Howell Science Complex, 1000 E. 5th Street
Greenville, NC 27858, USA; Tel: +252-328-4980; Fax: +252-328-0753 (dewittr@ecu.edu)

EDITORIAL BOARD

Ian K. Bailiff, Luminescence Dating Laboratory, Univ. of Durham, Durham, UK (ian.bailiff@durham.ac.uk)

Geoff A.T. Duller, Institute of Geography and Earth Sciences, Aberystwyth University, Ceredigion, Wales, UK
(ggd@aber.ac.uk)

Sheng-Hua Li, Department of Earth Sciences, The University of Hong Kong, Hong Kong, China (shli@hku.hk)

Shannon Mahan, U.S. Geological Survey, Denver Federal Center, Denver, CO, USA (smahan@usgs.gov)

Richard G. Roberts, School of Earth and Environmental Sciences, University of Wollongong, Australia
(rgrob@uow.edu.au)

REVIEWERS PANEL

Richard M. Bailey

Oxford, UK

richard.bailey@ouce.ox.ac.uk

James Feathers

Seattle, WA, USA

jimf@uw.edu

Rainer Grün

Canberra, Australia

rainer.grun@anu.edu.au

David J. Huntley

Burnaby B.C., Canada

huntley@sfu.ca

Sebastian Kreutzer

Aberystwyth University, UK

sebastian.kreutzer@aber.ac.uk

Michel Lamothe

Montréal, Québec, Canada

lamothe.michel@uqam.ca

Norbert Mercier

Bordeaux, France

norbert.mercier@u-bordeaux-montaigne.fr

Didier Miallier

Aubièrre, France

miallier@clermont.in2p3.fr

Andrew S. Murray

Roskilde, Denmark

anmu@dtu.dk

Vasilis Pagonis

Westminster, MD, USA

vpagonis@mcdaniel.edu

Naomi Porat

Jerusalem, Israel

naomi.porat@gsi.gov.il

Daniel Richter

Leipzig, Germany

drichter@eva.mpg.de

David C.W. Sanderson

East Kilbride, UK

David.Sanderson@glasgow.ac.uk

Andre Sawakuchi

São Paulo, SP, Brazil

andreas@usp.br

Ashok K. Singhvi

Ahmedabad, India

singhvi@prl.res.in

Kristina J. Thomsen

Roskilde, Denmark

krth@dtu.dk

Web coordinators: Joel DeWitt, Regina DeWitt

Article layout and typesetting: Regina DeWitt

Bibliography: Sebastien Huot

Safelight for OSL dating laboratories: a follow-up study

Reza Sohbati^{1*}, MyungHo Kook¹, Lars P. Pirtzel¹, Kristina J. Thomsen¹

¹ Department of Physics, Technical University of Denmark, Risø Campus, Roskilde DK-4000, Denmark

*Corresponding Author: reza.sohbati@pm.me

Received: January 31, 2021; in final form: March 3, 2021

Abstract

We introduce a new lamp for use in optically stimulated luminescence (OSL) dating laboratories. The lamp is based on an LED with the peak emission wavelength at 594 nm that was previously characterised as safe for both samples and operators by Sohbati et al. (2017). We demonstrate that 48 h exposure to this lamp, delivering a power density of $0.2 \mu\text{W}\cdot\text{cm}^{-2}$ at sample position, results in $1 \pm 3 \%$ loss in the infrared stimulated luminescence (IRSL) signal from clean K-rich feldspar grains. The loss in quartz OSL and K-feldspar post-IR IRSL signals is anticipated to be even smaller, given their lower bleaching rate at the lamp's peak wavelength (i.e. 594 nm). We reiterate the conclusion by Sohbati et al. (2017) that the illumination provided by such a lamp is desirable for OSL dating laboratories.

Keywords: Luminescence dating; Laboratory illumination; Safelight; Darkroom; LED

1. Introduction

Samples intended for optically stimulated luminescence (OSL) dating are usually sensitive to light. It is thus important that any inherent signal is preserved during sample preparation prior to measurement. An OSL laboratory lamp ("The Risø Safelight") has been designed to meet this objective, particularly when used with quartz and feldspar. The lamp makes use of the same LED that was identified as safe for both samples and operators by Sohbati et al. (2017). The peak emission wavelength of this amber-coloured LED at 594 nm is far from the feldspar infrared absorption reso-

nance at ~ 850 nm (Hütt et al., 1988) and close to the human eye's maximum spectral sensitivity at 555 nm (Pokorny, 1979). Consequently, it can provide better visibility at lower intensities than the more common red-coloured lamps with typical maximum emission at 625-700 nm (e.g., Lamothe, 1995; Berger & Kratt, 2008), while having effectively less impact on the trapped charge giving rise to the quartz fast-component OSL and feldspar infrared stimulated luminescence (IRSL) signals.

Sohbati et al. (2017) measured the bleaching effect of this LED at a power density of $\sim 12.7 \mu\text{W}\cdot\text{cm}^{-2}$, and calculated that 48 h exposure to it at a power density of $\sim 0.2 \mu\text{W}\cdot\text{cm}^{-2}$ should result in $\leq 1\%$ loss of IRSL signal at 50°C (IR_{50}) from clean K-rich feldspar grains. However, no measurement was carried out directly at $0.2 \mu\text{W}\cdot\text{cm}^{-2}$ to validate this conclusion. The purpose of this study is to directly quantify the bleaching effect of this new laboratory lamp on the K-feldspar IR_{50} signal at a power density of $\sim 0.2 \mu\text{W}\cdot\text{cm}^{-2}$ at sample position.



Figure 1. Photo of the lamp tested in this study.

2. Methods

The new lamp consists of an array of nine LEDs arranged in a ring inside a housing of die-cast aluminium alloy, covered by a stack of transparent (3 mm thick) and semi-transparent (1 mm thick) acrylic light diffusers at the front to enhance illumination uniformity. It is fitted with a user-adjustable power control allowing the output to be adjusted from 1.75 to 100% of full power (Fig. 1). The corresponding minimum and maximum power consumptions of the lamp are 0.3 and 3 W, respectively. Measurement of the light emission spectrum was undertaken using an Ocean Optics MAYA2000-Pro spectrometer, and the power density was determined with a THORLABS PM100D power meter console equipped with a S130C photodiode sensor. The distance between the lamp and the samples was ~1.7 m and the power density at sample position was set to $0.2 \mu\text{W}\cdot\text{cm}^{-2}$.

Two K-rich feldspar (i.e. $\rho < 2.58 \text{ g}\cdot\text{cm}^{-3}$) samples were tested: sample 146610 is a loess sample from South Island, New Zealand (Sohbati et al., 2016) that was originally among the samples tested by Sohbati et al. (2017), and sample H33052 is the K-rich feldspar fraction of a sand sample from a dune ridge in Rømø, Denmark. Risø calibration quartz is produced from the quartz fraction of this sample (Hansen et al., 2018).

Forty-eight small aliquots (~2 mm in diameter) from each sample were prepared by fixing the grains in stainless steel cups using Rüschi Silkospray silicone oil. Six of these were stored in the dark as a reference, while the rest were exposed for cumulative exposure periods of 3, 6, 12, 24, 48, 96 and 192 hours. Six aliquots were measured after each exposure period. In the case of sample H33052, eight aliquots were displaced during transportation. These are missing from exposure groups of 12 h (1 aliquot), 24 h (1 aliquot), 48 h (1 aliquot), 96 h (2 aliquots) and 192 h (3 aliquots).

All IR₅₀ L_n/T_n measurements were performed on a Risø TL/OSL Risø Model-DA-20 with an automated Detection And Stimulation Head (DASH) (Lapp et al., 2015). The IRSL signal was stimulated for 100 s using infrared diodes delivering a power density of ~175 $\text{mW}\cdot\text{cm}^{-2}$ at 850 nm, and measured through a blue filter pack composed of a 3-mm-thick Schott BG3 and a 2-mm-thick Schott BG39 filters. The preheat temperature was 250 °C, maintained for 60 s and the test dose size was ~1.2 Gy for all IRSL measurements. The heating rate was $5 \text{ }^\circ\text{C}\cdot\text{s}^{-1}$ during all thermal treatments. All L_n/T_n values were calculated using the first 1 s of the signals subtracted by the average of the last 10 s.

3. Results

The lamp emits at a peak wavelength of 594 nm, which is similar to that identified as being optimum by Sohbati et al. (2017). Output power was adjusted so that the power density at the position of the aliquots was $\sim 0.2 \mu\text{W}\cdot\text{cm}^{-2}$. According to the calculations by Sohbati et al. (2017), these conditions should result in $\leq 1\%$ loss of the K-rich feldspar IR₅₀ signal after 48 h. It is noteworthy to add that the IR₅₀ signal is

more easily bleached than the quartz OSL signal at the peak emission wavelength of the lamp (i.e. 594 nm), presumably because the feldspar IRSL trap photoionization cross section at this wavelength is greater than that of the source trap for the quartz fast-component OSL signal (Spooner, 1994a,b). This is supported by the results of Sohbati et al. (2017), who, on average, observed ~30% lower bleaching in the quartz OSL signal than the K-rich feldspar IR₅₀ signal from their samples exposed to this wavelength. Consequently, if we can establish the safety of the lamp using the IR₅₀ signal, we can be confident that it is also safe for use with the quartz OSL and the more-difficult-to-bleach K-feldspar post-IR IRSL signals.

The measured L_n/T_n values for both samples are summarised in Fig. 2. A visual inspection of the data indicates that there are a few outlying datapoints (Fig. 2). For the purpose of identifying and removing the outliers objectively and quantitatively, an outlier detection method using quantile regression (Breiman, 2001; Meinshausen, 2006) was applied to both datasets. In this approach, the conditional quartiles ($Q1$, $Q2$ and $Q3$) and the interquartile range (IQR) of all the observations (i.e. L_n/T_n values) are estimated within the range of the predictor variable (i.e. the exposure time) based on a quantile random forest of regression trees (Breiman, 2001; Meinshausen, 2006). The individual observations are then compared to the quantities $F1 = Q1 - 1.5 \times IQR$ and $F2 = Q3 + 1.5 \times IQR$ defined as outlier detection thresholds; the so-called “fences”. Any observation that is less than $F1$ or greater than $F2$ is considered an outlier. Using this approach, three and one outliers were detected in the 146610 and H33052 datasets, respectively (Fig. 2). These are excluded from further analysis and not included in calculating the bleaching rates.

To derive the bleaching rate of each sample individually, the data were fitted using the model by Bailiff & Barnett (1994) with the functional form of $I = I_0(1 + Bt)^{-P}$, where I_0 is initial intensity, t is exposure time, and B and P are constants such that $1 \leq P \leq 2$ (Fig. 3). For both samples, the resulting best-fit parameter values translate into an IR₅₀ signal loss of $1 \pm 3\%$ after 48 h of exposure to the lamp (Table 1).

4. Discussion

The K-rich feldspar IR₅₀ signal loss of $1 \pm 3\%$ calculated here is, within the error limits, consistent with the predicted value of $\leq 1\%$ previously reported by Sohbati et al. (2017). However, the calculated upper bound of 4% implies that, given the measurement and fitting errors, the apparent signal reduction can be as high as 4%. Sohbati et al. (2017) observed a difference up to ~14% ($n = 4$) in the bleaching rate of the K-feldspar samples tested in their study. It is thus curious that, despite their very different geological origin, depositional environment and grain size, both samples studied here appear to have similar bleaching rates. This may be due to the insignificant loss of the IR₅₀ signal and thus the limited range of the observed L_n/T_n values that hinder us from calculating the true bleaching rate of the two samples over these

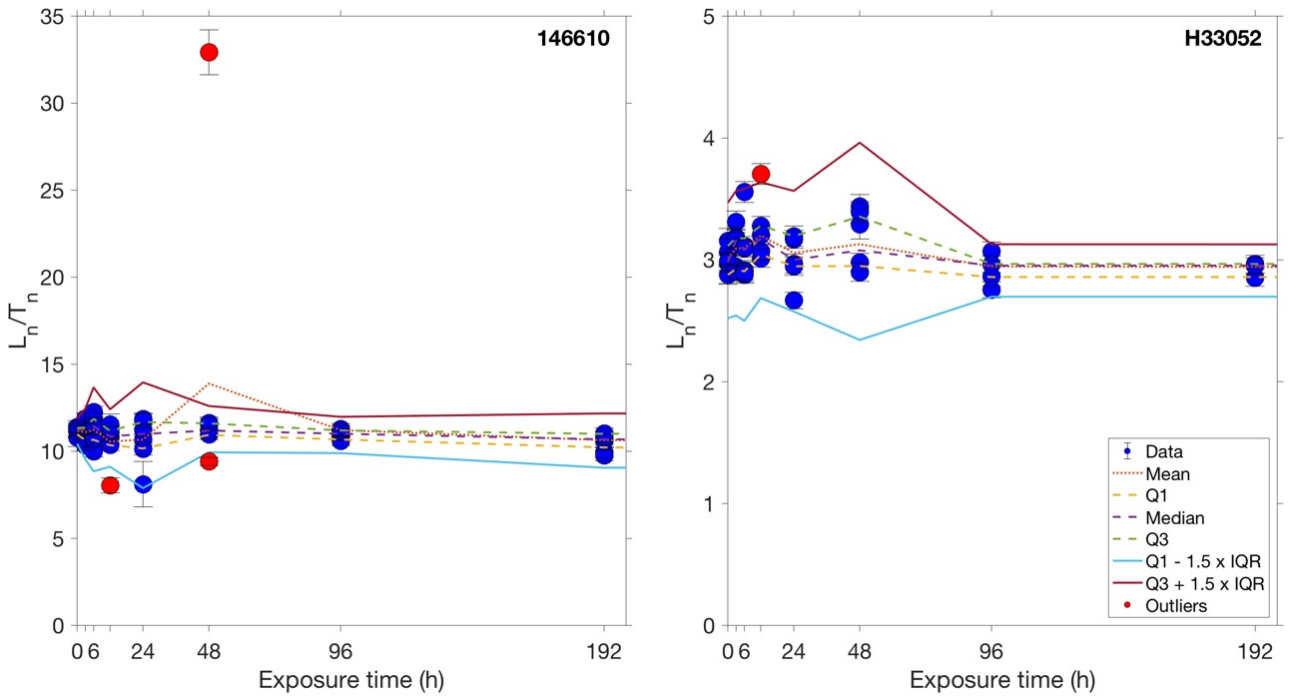


Figure 2. The IR₅₀ L_n/T_n measurements versus exposure time. Dashed lines indicate the first ($Q1$), the second ($Q2$ or median) and the third ($Q3$) conditional quartiles and the dotted lines show the mean. Solid lines represent the quantities $F1 = Q1 - 1.5 \times IQR$ and $F2 = Q3 + 1.5 \times IQR$ defined as threshold for outlier detection. Circles in red denote the detected outliers, which lie below $F1$ or above $F2$.

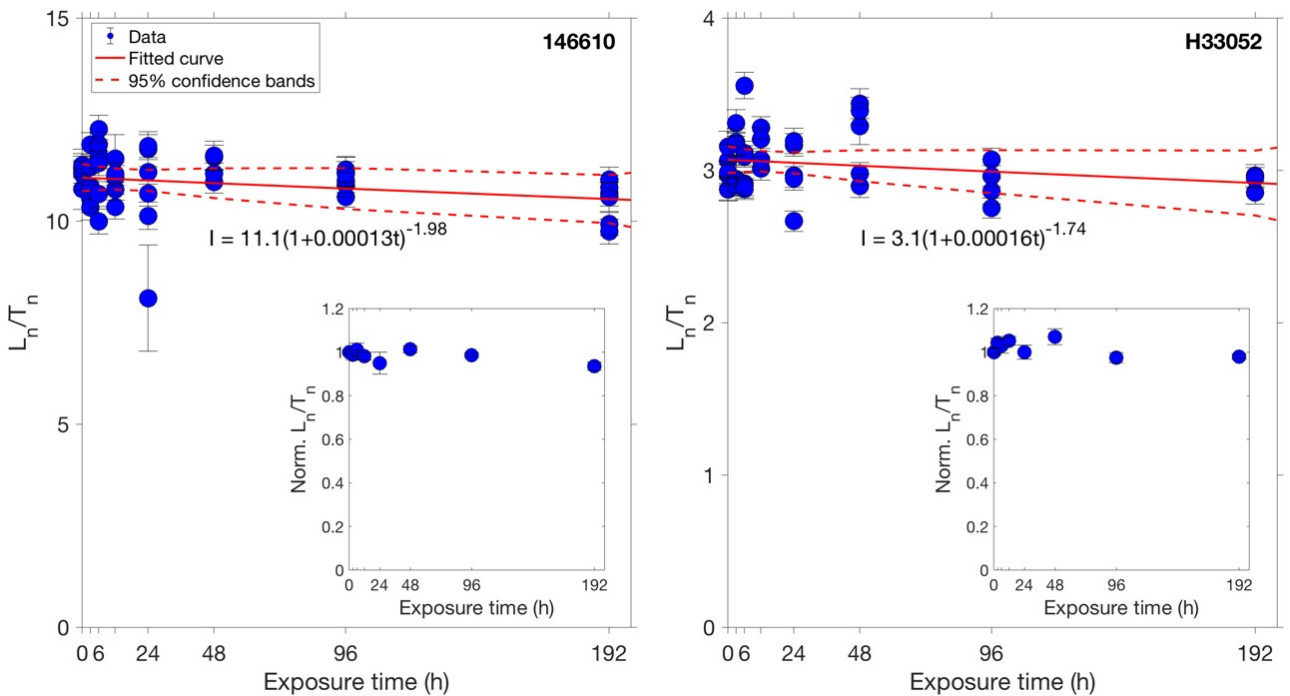


Figure 3. The same data as in Figure 2 excluding the outliers. Solid lines represent the best fit of the model by [Bailiff & Barnett \(1994\)](#) in the form of $I = I_0 (1+Bt)^{-P}$ to the data, and the dashed lines indicate the 95% confidence bands. The insets show the same data as in the main figures averaged and normalised to the corresponding data at $t = 0$.

Table 1. Summary of the samples, the best-fit parameter values, the goodness-of-fit statistics and the calculated signal loss after 48 h of exposure to the lamp. CB: confidence bounds, SSE: the sum of squares due to error, DFE: degrees of freedom, RMSE: root mean squared error.

| Sample name | Dose + se (Gy) | Grain size (μm) | I_0 [95% CB] | B [95% CB] | P [95% CB] | Predicted signal loss in % [95% CB] | Goodness-of-fit statistics [SSE, R-square, DFE, Adjusted R-square, RMSE] | Reference |
|-------------|-----------------|------------------------------|-------------------------|---------------------------------|--------------------------|-------------------------------------|--------------------------------------------------------------------------|---------------------|
| 146610 | 18.5 ± 4 | 40–63 | 11.07 [10.74, 11.41] | 0.0001297 [-0.0518, 0.05206] | 1.983 [-782.7, 786.7] | 1.22 [-3.32, 3.37] | [2.1029, 0.0590, 42, 0.0142, 0.2238] | Sohbati et al. 2016 |
| H33052 | 4.81 ± 0.07 | 180–250 | 3.07 [2.983, 3.158] | 0.0001553 [-0.0522, 0.05251] | 1.735 [-575.7, 579.1] | 1.28 [-3.35, 3.37] | [0.4164, 0.0546, 36, 0.0021, 0.1076] | Hansen et al. 2018 |

exposure times. It is notable that the observed signal loss in 146610 and H33052 after 192 h (i.e. 8 days) of exposure is only $6.48 \pm 2.02\%$ ($n = 6$) and $2.16 \pm 1.9\%$ ($n = 3$), and the corresponding values after 48 h are $-1.24 \pm 1.6\%$ ($n = 4$) and $-7.09 \pm 3.75\%$ ($n = 5$), respectively. Obviously, a more accurate and precise estimate of the bleaching rate requires substantially more datapoints, at much longer exposure times up to a few years; this was deemed neither practicable nor necessary for the purposes of this study.

5. Conclusions

Our new bleaching tests demonstrate that 48 h of exposure to the new laboratory lamp emitting at 594 nm with a power density of $\sim 0.2 \mu\text{W}\cdot\text{cm}^{-2}$ at the sample position results in a loss of $\sim 1\%$ in the IR_{50} signal from the K-rich feldspar samples investigated here. The loss of quartz OSL and K-feldspar pIRIR signals is anticipated to be even smaller than 1%, as they have a lower bleaching rate at the peak emission wavelength of the lamp (Sohbati et al., 2017). This is in line with the earlier conclusion by Sohbati et al. (2017), who established that such lighting conditions in OSL dating laboratories are optimum, as they are both safe for samples and provide a clear visibility for operators.

It is noteworthy that the 1%/48 h/0.2 $\mu\text{W}\cdot\text{cm}^{-2}$ IR_{50} signal loss calculated above is derived from clean K-rich feldspar grains that were directly exposed to the lamp. The signal reduction in dirty bulk samples and coated sand grains during the early steps of sample preparation such as sieving and HCl acid treatment is anticipated to be even lower. Furthermore, the total cumulative exposure time to laboratory light during most routine sample preparation procedures is usually much shorter than 48 h. Thus, if necessary, the operator could afford using higher power densities (e.g. by up to a factor of 2) for shorter durations, during high-risk sample preparation steps such as HF treatment. Finally, regardless of how small the bleaching effect of a safelight, the common-sense advice is to keep the exposure of OSL samples to any light source to an absolute minimum prior to measurement of the natural signal.

Acknowledgements

The authors would like to thank Vicki Hansen for sample preparation and Naomi Porat for useful comments that helped improve this manuscript.

References

- Bailiff, I. K. and Barnett, S. M. *Characteristics of infrared-stimulated luminescence from a feldspar at low temperatures*. Radiation Measurements, 23: 541–545, 1994. doi: 10.1016/1350-4487(94)90096-5.
- Berger, G. W. and Kratt, C. *LED laboratory lighting*. Ancient TL, 26(1): 11–14, 2008.

- Breiman, L. *Random Forests*. Machine Learning, 45: 5–32, 2001. doi: 10.1023/a:1010933404324.
- Hansen, V., Murray, A., Thomsen, K., Jain, M., Autzen, M., and Buylaert, J.-P. *Towards the origins of over-dispersion in beta source calibration*. Radiation Measurements, 120: 157–162, 2018. doi: doi.org/10.1016/j.radmeas.2018.05.014.
- Hütt, G., Jaek, I., and Tchonka, J. *Optical dating: K-feldspars optical response stimulation spectra*. Quaternary Science Reviews, 7: 381–385, 1988. doi: 10.1016/0277-3791(88)90033-9.
- Lamothe, M. *Using 600-650 nm light for IRSL sample preparation*. Ancient TL, 13: 1–4, 1995.
- Lapp, T., Kook, M., Murray, A. S., Thomsen, K. J., Buylaert, J.-P., and Jain, M. *A new luminescence detection and stimulation head for the Risø TL/OSL reader*. Radiation Measurements, 81: 178–184, 2015. doi: 10.1016/j.radmeas.2015.02.001.
- Meinshausen, N. *Quantile Regression Forests*. Journal of Machine Learning Research, 7: 983–999, 2006.
- Pokorny, J. (ed.). *Congenital and Acquired Color Vision Defects*. Grune & Stratton, 1979.
- Sohbati, R., Borella, J., Murray, A., Quigley, M., and Buylaert, J. *Optical dating of loessic hillslope sediments constrains timing of prehistoric rockfalls, Christchurch, New Zealand*. Journal of Quaternary Science, 31: 678–690, 2016. doi: 10.1002/jqs.2895.
- Sohbati, R., Murray, A., Lindvold, L., Buylaert, J.-P., and Jain, M. *Optimization of laboratory illumination in optical dating*. Quaternary Geochronology, 39: 105–111, 2017. doi: 10.1016/j.quageo.2017.02.010.
- Spooner, N. A. *On the optical dating signal from quartz*. Radiation Measurements, 23: 593–600, 1994a. doi: 10.1016/1350-4487(94)90105-8.
- Spooner, N. A. *The anomalous fading of infrared-stimulated luminescence from feldspars*. Radiation Measurements, 23: 625–632, 1994b. doi: 10.1016/1350-4487(94)90111-2.

Reviewer

Naomi Porat

Methods Note: Can hydrogen peroxide digestion of organic matter ever be too aggressive for OSL dating?

Kenneth Lepper^{1*}, Jenna Fischer^{1,2}

¹ Optical Dating and Dosimetry Laboratory, Department of Geosciences, North Dakota State University, P.O. Box 6050 / #2745, Fargo, ND 58108-6050

² Mine Geologist, Coeur Mining at Wharf Resources LLC, 10928 Wharf Rd, Lead, SD 57754

*Corresponding Author: Ken.lepper@NDSU.edu

Received: April 14, 2021; in final form: April 23, 2021

1. Introduction

Removal of organic matter and digestion of organic residues is a ubiquitous step in sample processing for luminescence dating (Aitken, 1998). Macroscopic organic debris, if present, is largely captured during grain-size sieving. Most, if not all, laboratories use a hydrogen peroxide (H_2O_2) treatment to digest microscopic organic debris and organic residues. It is not uncommon for samples, even samples collected from C-horizons, to react mildly or moderately to H_2O_2 at reagent concentration (30% solution) for a period of up to a few hours. Occasionally samples are encountered that react rapidly and vigorously to H_2O_2 or, conversely, samples that seem to have a delayed reaction; not reacting immediately but after several hours of soaking in H_2O_2 . The collective experience of numerous luminescence dating labs indicates that these “normal” reactions to H_2O_2 treatment do not have a significant impact on the resulting measured TL/OSL signals or D_e distributions; thus the ubiquitous use of H_2O_2 digestion.

Recently we processed a set of samples that reacted so intensely and for such a prolonged period that we questioned, “Can H_2O_2 digestion of organic matter ever be too aggressive for OSL dating?” One of the samples provided an opportunity to experimentally evaluate that question. The sample set comes from a strandplain (or ridge and swale) shoreline sequence bordering Lake Claire in northeastern Alberta, Canada. Tar sands are mined in this region and notably so upstream along the Athabasca River. However, based on the estimated ages of the samples and geomorphological interpretations, it was not anticipated that significant amounts of tar sands would have been incorporated into the ridges that were sampled (Zamperoni et al., 2017). Even if the samples did contain some sand grains and/or bitumen derived

from the tar sand deposits, it still must be removed and H_2O_2 treatment is the standard.

2. Treatments and Observations

It is important to state that the personnel conducting the treatments described herein all had received university level chemical safety training as well as luminescence dating laboratory specific safety training. The recommended PPE was worn at all times and the HF treatments described later were conducted in an HF compliant fume hood and with a safety spotter monitoring at all times.

In our laboratory we generally treat 10–20 cm³ of sieved sediment with 25–50 ml of 30% H_2O_2 solution. The first two Lake Claire samples processed reacted very vigorously with H_2O_2 and required spent solution to be decanted and fresh H_2O_2 to be introduced at least twice. Although the reactions were vigorous and somewhat prolonged, they were not exceedingly beyond past experiences, so the reactions were noted on a sample data sheet and work proceeded to the third sample.

When H_2O_2 was added to the third sample the initial reaction was shockingly violent with profuse bubbling and prodigious emission of gas for both the 90–150 μ m and the 150–250 μ m size fraction. The reaction was slowed/cooled by adding DI water. When the reaction subsided the solution was decanted and fresh H_2O_2 added. The reaction immediately resumed its former violence. At this point the sample was placed in a reaction safe cabinet and allowed to spend the available H_2O_2 . The H_2O_2 was refreshed twice a day for 4 days. Each time the spent solution was decanted, it was milky or silty, even though prior to adding fresh H_2O_2 we would rinse the sample in DI water until the decanted water was clear. During the four days of decanting and adding fresh

H₂O₂ we took a subsample out of the OSL lab where it could be examined under normal lighting and indeed there were black sand-sized grains present. Although these can typically be seen under lab lighting, it is not uncommon for beach deposits to contain grains of biotite, amphibole, or magnetite. So, the presence of a small proportion of black grains was not considered unusual at the start of the project. Additionally, on the fourth treatment day the reaction had slowed to a level where we could visually see the top and sides of the beaker. We noticed that gas was being released from discrete foci throughout the sediment and traveled toward the surface in vertical bubble streams or jets where they erupted (see supporting video). Our interpretation of the various observations during processing of this sample is that it did include a proportion of sand-size particles that were aggregates of smaller particles cemented by bitumen and likely sand grains with bitumen surface coatings as well. The most likely source of these particles and grains is erosion of tar sands far prior to industrial activities in the region.

To evaluate the impact of the H₂O₂ processing we created subsamples or batches in the 90–150 μm (VFS) and 150–250 μm (FS) size-fraction that were treated in different manners. Batch 0 (FS) was the original sample that spent over 4 days in twice daily refreshed 30% H₂O₂ solution. Batch 1 (VFS) were treated as normal by direct digestion in the H₂O₂ solution for ~16 hours. Batch 2 (VFS) was mechanically disaggregated prior to H₂O₂ treatment. Batch 3 (FS) samples were treated with Acetone to dissolve bitumen.

Batch 2 samples were placed in a very low concentration (5 mmol) solution of sodium pyrophosphate dispersant with a magnetic spin bar. It was agitated with the spin bar in this solution for ~16 hours to promote break down of bitumen cemented fine-grained aggregates. Of course, the supernatant liquid was very cloudy or milky. The sample was rinsed in DI water until the decanted rinsate was clear. Fresh dispersant solution was added and the sample was again agitated with the spin bar for an additional 8 hours. At this stage the supernatant liquid was only slightly cloudy. The sample was

rinsed and we proceeded to a standard H₂O₂ treatment (30% solution). The reaction was vigorous, but significantly subdued compared to batch 0 and 1.

Batch 3 was treated with 90% acetone and agitated with a magnetic spin bar for ~16 hours. After this treatment the solution (waste acetone) was extremely dark in appearance. The sample was rinsed in fresh acetone twice, after which the rinsate was essentially clear. No additional treatments for organic removal were conducted on batch 3.

Following these treatments for organic matter all grain-size fractions were processed in the same manner to obtain clean quartz for OSL measurement (HCl, HF, post-HF rinses; see supplement to Lepper et al. 2007 for details). All sample batches in this study reacted vigorously with HF generating noticeable heat and gas. One might expect that batch 1, because of a shorter H₂O₂ treatment, may have reacted much more vigorously with HF than the other batches. However, based on our observations, that was not the case.

The prepared sand from all batches was measured using a Risø DA-15 TL/OSL reader system. The system is equipped with a 40 mCi 90Sr/90Y β-source for dose calibrations, which irradiated at a rate 0.113 Gy/s at the time of the experiments. Luminescence was stimulated with blue light (470 ± 30 nm) from a diode array and measured with an EMI model 9235QA PMT in the UV emission range (5 mm Hoya U-340). OSL SAR data collection procedures were used (Murray & Wintle, 2000) with a uniform cut heat and preheat of 160 °C for 10s throughout the SAR process (Lepper et al., 2000; Wintle & Murray, 2006). The SAR procedures used included four regeneration doses. Dose response calibration was conducted for every aliquot and it was linear within the regeneration dose range used. Ninety-six (96) individual aliquots were analyzed from each batch in this study. Prepared aliquots have been estimated to contain approximately 300 grains. Data was mildly filtered following the criteria described in Lepper et al. (2003; 2007 supplement) resulting in D_e data sets ranging from n = 94 to 96 aliquots for analysis and comparisons.

Table 1. Summarized conditions and results of this study.

| Batch ID - grain size | Organic Removal Treatment | n ¹ | M/m ² | v _t ³ | Data Mean D _e (Gy) | Freq. Dist. Mean D _e (Gy) |
|-------------------------------|-----------------------------------------------------------------------------------------------------|----------------|------------------|-----------------------------|-------------------------------|--------------------------------------|
| Batch 0 - FS | Over 96 hour soak in 30% H ₂ O ₂ | 94/96 | 1.01 | 11.10% | 12.95 ± 0.15 | 12.97 ± 0.09 |
| Batch 1 - VFS | ~ 16 hour soak in 30% H ₂ O ₂ (control) | 94/96 | 1.01 | 10.50% | 13.11 ± 0.14 | 13.01 ± 0.14 |
| Batch 2 - VFS | 24 hours continuous aggitation in dispersant prior to 16 hour soak in H ₂ O ₂ | 96/96 | 0.97 | 13.50% | 12.74 ± 0.18 | 13.06 ± 0.24 |
| Batch 3 - FS | ~ 16 hour continuous aggitation in Acetone; no H ₂ O ₂ | 95/96 | 0.98 | 12.40% | 13.06 ± 0.17 | 13.06 ± 0.19 |
| Mean ± group std. dev. | | | | | 12.98 ± 0.18 | 13.03 ± 0.05 |

¹No. of aliquots used for OSL D_e calculation / no. of aliquots from which OSL data was collected (filtering criteria given in Lepper et al., 2003)

²Mean/median ratio: a measure of dose distribution symmetry/asymmetry (see supplement to Lepper et al., 2007).

³Total dose distribution data dispersion (Std. dev./mean).

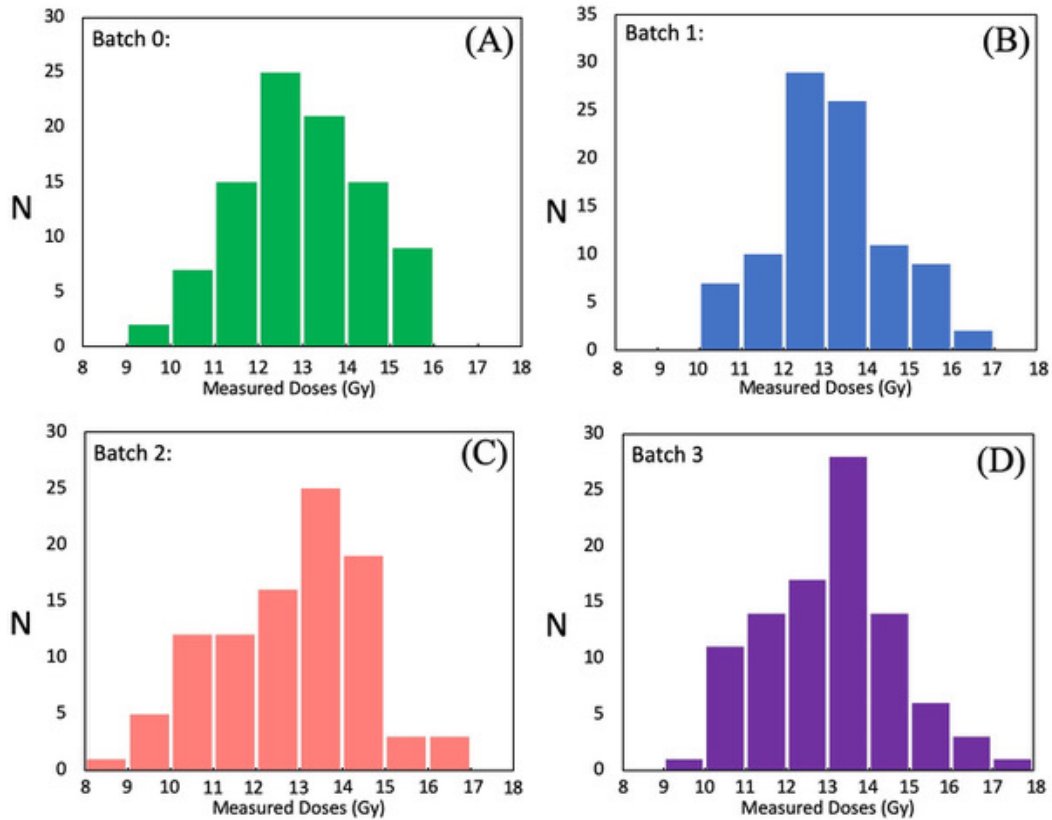


Figure 1. D_e data histograms for each treatment group/batch (A) Over 96 hour soak in H_2O_2 (B) ~ 16 hour soak in H_2O_2 (C) ~ 16 hours of agitation in dispersant prior to H_2O_2 (D) ~ 16 hours of continuous agitation in acetone; no H_2O_2 treatment.

3. Results

Table 1 shows the treatment groups for which OSL SAR measurements were made, the organic removal treatment received, the mean and std. err. of the individual D_e data sets that were derived from both the data and from fitting the data with a single Gaussian population model, as well as some additional parameters that our lab uses to characterize or evaluate dose distributions. Figure 1 shows the D_e data histograms for each batch and Figure 2 shows the derived frequency distributions from the Gaussian models for the treatment groups. As can be seen there is virtually no difference among the treatments and no statistically significant difference in mean D_e among the treatment groups evaluated (Table 1). All D_e distribution means are within one 1 std. dev. of their group mean when considering their respective errors.

Batch 1, which had no agitation and the shortest H_2O_2 soak time, had the lowest data dispersion (ν_t in Table 1) reflected as the narrowest frequency distribution (Figure 2) but, again, it is not statistically significant. The data histogram for batch 2 and to some degree batch 3 have a suggestion of more lower D_e values (Figure 1). Both of these batches underwent an extended period of mechanical agitation during the organic removal treatments. Both of these batches, 2 and 3, also have higher data dispersion (ν_t in Table 1) than batches 0 and 1. Similarly batches 2 and 3 have mean/median

ratios (M/m in Table 1) of less than 1.00, which quantifies a slight skew to lower D_e values. A perfectly symmetric distribution has a M/m value equal to 1. However, the differences in these parameters from batch to batch and the difference from ideal behavior is subtle and within normal ranges ob-

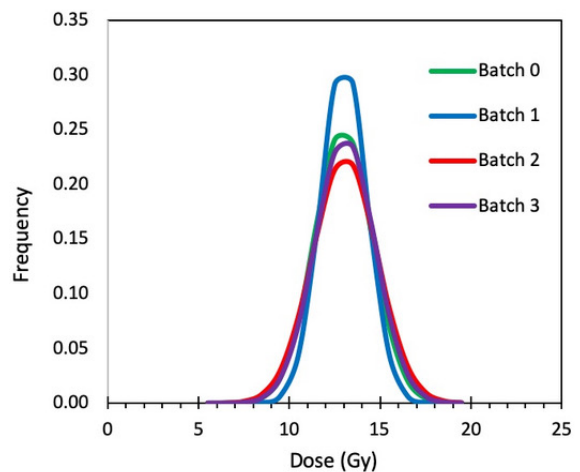


Figure 2. Frequency distributions derived from the Gaussian models for the treatment groups/batches.

served in other projects.

This small experiment also highlights the use of acetone to dissolve oily residues and grain coating from sands. Acetone dissolution could be used as part of the pre-processing of bituminous sands for luminescence dating. However, it may be advisable to develop a procedure that does not require an extend period of mechanical agitation in the acetone.

4. Conclusions

Despite alarmingly vigorous reactions, our data suggests that direct digestion of organic matter with a reagent grade 30% solution of H₂O₂, even for samples containing a noticeable fraction of bitumen, does not result in a significant or deleterious impact on D_e determinations. Although not a statistically robust conclusion, some quantifiable parameters suggest that prolonged periods of stirring in liquid (mechanical agitation) may not be advisable. Acetone may provide an alternative to hydrogen peroxide when removing oily residues and bitumen from sand samples.

References

- Aitken, M. *An Introduction to Optical Dating*. Oxford University Press, New York, 1998.
- Lepper, K., Agersnap-Larsen, N., and McKeever, S. *Equivalent dose distribution analysis of Holocene eolian and fluvial quartz sands from Central Oklahoma*. *Radiation Measurements*, 32: 603–608, 2000.
- Lepper, K., Wilson, C., Gardner, J., Reneau, S., and Levine, A. *Comparison of SAR techniques for luminescence dating of sediments derived from volcanic tuff*. *Quaternary Science Reviews*, 22: 1131–1138, 2003.
- Lepper, K., Fisher, T., Hajdas, I., and Lowell, T. *Ages for the Big Stone Moraine and the oldest beaches of glacial Lake Agassiz: Implications for deglaciation chronology*. *Geology*, 35: 667–670, 2007. doi: 10.1130/G23665A.1.
- Murray, A. and Wintle, A. Q. O. *Effects of thermal treatment and their relevance to laboratory dating procedures*. *Radiation Measurements*, 32: 387–400, 2000. doi: 10.1016/S1350-4487(00)00057-3+.
- Wintle, A. and Murray, A. A. *review of quartz optically stimulated luminescence characteristics and their relevance in single-aliquot regeneration dating protocols*. *Radiation Measurements*, 41: 369–391, 2006. doi: 10.1016/j.radmeas.2005.11.001.
- Zamperoni, A., Johnston, J., Wolfe, B., Hall, R., Lepper, K., Jol, H., Endres, T., and Duguay, C. *Characterizing relict shorelines to establish the most detailed account of lake-levels in the Peace Athabasca delta: A key hydrologic node of the Mackenzie River basin, northwestern Canada*. *GSA Proceedings with Abstracts*, 49: 2, 2017. doi: 10.1130/abs/2017NE-290049.

Reviewer

Christina Neudorf

Reviewer comment:

I've wondered about the potential effect of chemical treatments on measured D_e values from sediments. This short methods note shows encouraging results. Several questions could be addressed in a future in-depth study.

I wonder if the exothermic reaction attained during HF treatment of quartz leads to a similar temperature increase of the sample as the H₂O₂ treatments in this study. It would be interesting to know if perhaps a larger difference in measured D_e (or signal intensity) would be observed with and without H₂O₂ treatments, if the sample was not subsequently treated with HF (as is sometimes done with feldspar). Also, more detailed data analysis could show the effect the various treatments have on signal sensitivity. If sample treatments do lead to changes in signal sensitivity, this may have an impact on signal counting statistics, dose distributions and final D_e error.

Thesis Abstracts

Index

| | |
|---------------------|-------|
| Kartika Goswami | p. 10 |
| Dirk Mittelstraß | p. 11 |
| Mahadev Rawat | p. 12 |
| Svenja Riedesel | p. 12 |
| Maria Schaarschmidt | p. 13 |
| Atul Kumar Singh | p. 14 |
| Giulia Tamburini | p. 15 |

Kartika Goswami

Luminescence chronology of the fluvial archives from the Kaveri Basin, India: Implications to late Quaternary climate change

February 2021

Indian Institute of Science Education and Research Kolkata,
Kolkata, India

Degree: Ph.D.

Supervisor: Dr. Manoj Kumar Jaiswal

The study uses optically stimulated luminescence (OSL) dating to reveal the chronology of the flood and deltaic sediments from the Kaveri basin, south India, and investigates the relationship of the sediment depositional history with the late-Quaternary climate changes. This objective is addressed by collecting flood deposit samples from the upper Kaveri basin, and the coastal/deltaic sediments from the coastal part of Kaveri delta, southeast India. The OSL ages are correlated with independent age controls such as radiocarbon (^{14}C) dating and young ages with the river gauge records, whenever possible. The quartz grains from southern India generally have bright OSL signal. This was advantageous in the dating of extremely young sediments. However, the river Kaveri flows mostly through rocky terrain in its upper reaches and is also joined by various tributaries. It therefore carries locally weathered sediments. Hence, it was interesting to explore the extent of bleaching, and thus the feasibility of OSL dating young flood sediments (~ few tens of hundreds of years only).

Heterogeneous bleaching was observed in the flood sediments from the upper parts of Kaveri. Age estimates were made using existing age models, like the minimum age model (MAM) and the central age model (CAM). Additionally, grain size analysis, micropaleontological studies (of deltaic sediments), and palaeodischarge analysis using the slope-area method (from flood deposits) are applied to further reach our research goals.

The study of the flood deposits, provided insights into the monsoon flood-climate relationship. The study revealed that high-magnitude flooding events have occurred during major climatic shifts, from fluvial dormancy to sudden outburst of monsoons (~ 2 ka), from warmer to colder periods (onset of 'Little Ice Age' (LIA) ~ 14th century), from colder to warmer periods (end of LIA ~ 19th century) and ~ 20th century. This also indicates that not all wet phases are associated with large floods and not all dry phases with low floods or droughts. The study also demonstrated that the occurrence of the 20th century floods in the upper reaches of Kaveri is a result of high-intensity, short-duration storms. Brief precipitation analysis of the recent 2018 Kerala/Karnataka floods suggests that it is not only the increased amount of rainfall but also the temporal variability in the downpour that affects the occurrence of floods in the study area. Additionally, the paleodischarge analysis points out that the floods in recent times (post 1950) are occurring at a higher magnitude than the paleofloods.

The OSL ages, and the micropaleontological results obtained from the four deltaic subsurface sediment cores of 25 m depth each, revealed a close correlation of the sedimentary dynamics of the Kaveri river with the late-Quaternary sea-level and accompanied warmer conditions. The river has attempted to re-establish its equilibrium profile with the rise in the sea-level during ~ 140–143 ka, ~ 121 ka, ~ 95–100 ka, ~ 81–89 ka, ~ 73–78 ka, ~ 57–60 ka, ~ 40–45 ka, 6–9 ka, ~ 5 ka, and ~ 3 ka. This is majorly achieved by the river's vertical aggradational deposition as a result of a balanced influx of fluvial sediment with sea-level rise. However, a gradual progradation of the coastline towards the sea since ~ 30–15 ka is also observed, suggesting the effect of gradually falling sea-level in the coastal stratigraphy during this period. At ~ 6–9 ka, ~ 45 ka, ~ 75 ka, and ~ 121 ka, the presence of foraminifers is also observed in these coastal shores, suggesting marine influence. However, ~ 6–9 ka transgression is seen as the most pronounced and long-lived in the study area out of them all. Luminescence chronology of the cores also hints towards a fault movement post ~ 70 ka, indicating the role of Pleistocene tectonics, sea-level changes, climate, river dynamics in the late-Quaternary evolution of the Kaveri delta.

Therefore, the findings of present work contribute to the understanding of the regional palaeo-climate and its implications to the fluvial responses from the Kaveri basin, southeast India.

Dirk Mittelstraß

Decomposition of weak optically stimulated luminescence signals and its application in retrospective dosimetry of quartz

December 2019

Institut für Kern- und Teilchenphysik, Technische Universität
Dresden, Dresden, Germany

Degree: M.Sc.

Supervisors: Arno Straessner, Johannes Heitmann

The accuracy of quartz CW-OSL dating results relies strongly on the dominance of the thermally stable and easy-to-bleach ‘fast’ signal component. If this component does not dominate the initial signal, systematic errors are likely. These are caused by signal components from insufficiently bleached or thermally unstable traps. A signal component separation procedure would solve this issue, but has to meet the following requirements to be applicable in daily lab routine:

1. Allow automated component and dose evaluation, without inherent need for user interaction.
2. Identify the number of components and their decay constants on a sample-to-sample basis.
3. Allow component-resolved dose calculation, even for samples with low-SNR measurements.
4. Be applicable for a large variety of instrumental and measurement conditions.

To fulfill these requirements, a new mathematical approach is presented. The signal component separation is divided into two major steps. In the first step, the number of signal components and their decay rates are identified. This is done by creating one global average CW-OSL curve from all measurements in a given data set. On this representative CW-OSL curve, the multi-component exponential decay fitting algorithm described by Bluszcz and Adamiec in 2006 is applied. In the second step, the signal component intensities for each single CW-OSL measurement are obtained by an algebraic decomposition algorithm, novel in the field of luminescence dating. The algorithm is purely analytical and based on linear algebra methods. This ensures mathematical robustness and allows the propagation of uncertainty. All algorithms were realized in R and bundled in an R package. Multiple simulations as well as some application tests are realized as Rmarkdown scripts and are therefore easy to reproduce.

Method parameters as well as the accuracy, precision and robustness of the procedures were tested at 10368 (step 1) respectively 15.5 million (step 2) simulated CW-OSL curves with varying detection- and component parameters. The step 1 simulation demonstrated a high reliability in identifying the fast component. In 97.4% of the 5184 relevant OSL curves, the estimated fast component decay rate is within $\pm 10\%$ of the true value. The correct number of components was found

in 73% of the OSL curves. Under-fitting (missing components) occurred in 21% of the simulated cases but found to be unproblematic for the decay rate estimation of the remaining components. Over-fitting (imaginary components) occurred in 6% of the cases and lead to shifted decay rates and therefore to systematic errors. As over-fitting is correlated to long measurement durations, it is recommended to limit them to 40 s. Typical background signal levels were found to have no significant impact on the decay rate accuracy. The step 2 simulation demonstrated high precision and 100% reliability in estimating the fast and medium component intensities. This reliability accounts also for the statistical error values. Slow component intensities, however, are systematically shifted in the presence of detection background signals. The introduction of a background component was tested. It removed these systematic errors but lead to highly imprecise slow component estimations in some cases due to the similar appearance of slow components and background signals.

As application test, five CW-OSL SAR quartz sample data sets were analysed. All samples were from different locations and had independent age control available. For two samples, for which the default late background subtraction analysis lead to under-estimated ages, the new approach found ages in accordance with the independent age control. For two other samples with also under-estimated ages, this was not the case. But for these samples the under-estimation could be related to other sample-specific issues. For the fifth sample, the already as correct classified CW-OSL age was confirmed.

As second application test, the no-heating SAR protocol proposed by Roberts et al. in 2018 was tested by dose recovery tests at two samples. For the coarse grain reference quartz ‘Las Sables’, the recovered dose was accurately estimated while for the dim fine grain quartz BT1713 the recovered dose was highly over-estimated. Both samples have similar OSL characteristics at room temperature with the ‘fast’ component becoming the medium component of five components.

The thesis shows, that the presented component separation method fulfills the defined requirements although the range of applicable measurement conditions remain to be further specified. Nonetheless, the usefulness of the method as reliable and rapid data analysis tool in quartz OSL dating is demonstrated.

The thesis is available for download at https://iktp.tu-dresden.de/IKTP/pub/19/Dirk_Mittelstrass_Master.pdf. A further improved version of the R package ‘OSLdecomposition’ and a tutorial are available at <https://luminescence.de/>.

Mahadev Rawat

**Late Holocene Evolution of Fluvial System in
Tamilnadu, India: Implications to Climate and Tectonics**

March 2021

Department of Earth Sciences, Indian Institute of Science
Education and Research Kolkata

Degree: Ph.D.

Supervisor: Dr. Manoj Kumar Jaiswal

Paleo-flood is one of the extreme events, also an essential fluvial archive preserving signatures of intense precipitation linked with climate changes. However, it remains a puzzle to be taken as a proxy for intense humid phases. Usually, humid periods are associated with high discharge, high-frequency flooding, whereas dry climate is associated with low discharge and low frequency of such extreme events. However, even dry periods are related to extreme events making it complicated. The study of paleo-flood requires a robust paleoflood record and precise geochronology beyond historical or instrumental records. The current work proposes exploring these events and thus constructing past flooding history by analysing the various fluvial deposits. The Palar, Gingee, Then-Pennai, Vellar and Lower and Kaveri River and its tributary as Amravati River in Southern India, Tamilnadu was chosen for the study. These rivers receive winter monsoon as a significant source of precipitation. Being as a low discharge river in rocky terrain, these are sensitive to high precipitation events.

Luminescence dating is a widely accepted and popular method for estimating the age of sediment burial. However, sediments' partial or heterogeneous bleaching poses a problem in dating the young sediments (< 2 ka). Except for the Kaveri River, all others are ephemeral river systems, flowing for a few hundred kilometres through the rocky terrain and having a high chance of mixing unbleached weathered sand grains. Bleaching and mixing can be further enhanced by short transportation distance. Application of various luminescence age models is required to get the best age estimate for such extreme events. This study aims to test luminescence dating feasibility in a system consisting of high energy fluvial deposits, where partial bleaching could be high.

All the samples were processed for OSL dating; the quartz grains are showing relatively low sensitivity in Gingee, Vellar and Amravati rivers and high sensitivity in the lower Kaveri River, equivalent to the calibration quartz. However, most of them suffer from partial bleaching. With the application of various luminescence age models, three sets of OSL ages were obtained. The first set (100 to 200 years BP) indicates a drastic change in climatic conditions associated with the recurring tropical cyclonic systems, which have resulted in high-frequency flooding events in recent time. The second set of OSL ages suggests a large scale flooding event between 700–800 years BP coinciding with the change of Medieval Warm Period (MWP) to the Little Ice Age (LIA). The third set of OSL age (2 ka to 3.5 ka) shows a shift in the Inter-Tropical Convergence Zone (ITCZ). The study suggests in-

creased flooding in a transition zone and not in a prolonged phase of either dry or humid periods.

Earlier the southern part of the Indian Peninsula has been thought to be a tectonically stable shield area. However, the research carried out during the past three decades indicates possible unstable tectonism, at least since the Jurassic. The fluvial system in continental records response swiftly to tectonics or climate changes. The tectonic and geomorphic processes are related to each other, and the effect of change in tectonic or climate can be easily seen in the drainage systems. The current study focuses on reconstructing the Holocene evolutionary history of the Gingee and the Vellar River basin. Physiography, drainage patterns, geomorphic features, and structural controls of the Gingee and the Vellar rivers were evaluated to reconstruct the drainage basin's evolutionary history.

The morphometric approach was applied to get the tectonic signal from the Gingee and Vellar River basins. The study helped in understanding the role of tectonic elements in the evolution of the basins. The literature survey and the morphometric analysis results have been applied to obtain information about the tectonic elements and the possible reconstruction of their activity in recent times. The analysis indicates the southward tilting of the Gingee drainage systems and northward tilting of the Vellar drainage systems, strong asymmetry in some reaches, pronounced elongation of certain tributaries. All these analyses and the previous studies point towards active tectonism in the area. Because of the tilting, the Gingee River is migrating towards the south and the Vellar River towards the north, leaving their paleochannels towards the north and south, respectively. The Gingee River migrated clockwise to its current position during the mid-Holocene period ~ 3.5 ka. The Vellar River got shifted in an anticlockwise direction during 1.28 ka BP. Luminescence ages of the paleochannels also suggest that both the rivers are migrating with the same rate of ~ 4.5 km/ka.

A PDF of this thesis can be requested by contacting mahadevgly@gmail.com

Svenja Riedesel

**Exploring variability in the luminescence properties of
feldspars**

January 2021

Department of Geography and Earth Sciences, Aberystwyth
University, Aberystwyth, United Kingdom

Degree: Ph.D.

*Supervisors: Prof Helen M. Roberts, Prof Geoff A.T. Duller,
Prof Nick J.G. Pearce*

Feldspars are the most abundant minerals in the Earth's crust and they have the ability to store charge within defects in their crystal lattice over geological time scales. This allows their use as natural dosimeters in luminescence dating studies, which enables chronologies of past geomorphological, geological and archaeological events to be established.

Despite the routine use of feldspars in luminescence dating studies over the past decades, many key questions regarding the physical processes leading to luminescence of feldspars remain unanswered. For example, the crystal defects functioning as electron trapping centres in feldspars are still unknown, and the causes of variability seen in anomalous fading rates of the blue emission (~410 nm) in feldspars have not been fully identified. Since feldspars are complex framework silicates with a variety of chemical compositions and mineralogical properties, linking properties inherent to the feldspar to particular luminescence characteristics is challenging. This thesis aims at establishing a better understanding of potential relationships between feldspar chemical composition, structural state and the number of phases present within a crystal and the luminescence properties of selected feldspar samples. To achieve this goal, this thesis investigates the luminescence properties of a selection of single crystal feldspars and feldspars of grain mixtures extracted from sediment and bedrock, by using a combination of excitation and emission spectroscopy, photo- radio-, thermo- and infrared stimulated luminescence and anomalous fading measurements.

Electron trap depths ranging from 2 eV to 2.4 eV were found in chemically and structurally different feldspars. The IR resonance peak, likely reflecting the first excited state of IR-sensitive electron trapping centres, is located 1.45 eV above the ground state of the trap. Similarities in energies measured for the ground and excited state energies across the sample suite indicate that defects functioning as electron trapping centres are likely located on the Si,Al-framework. Site-selective infrared photoluminescence (IRPL) excitation-emission spectroscopy revealed up to three different lattice environments in which the investigated electron trapping centres might be located. A comparison of chemically and structurally different alkali feldspars indicated the presence of K⁺ ions on M sites as one likely influence of the lattice environment of electron trapping centres in feldspars. Disorder of the tetrahedral site occupancy of Al³⁺ ions has only little effect on electron trapping centres and related IRPL emissions, and no correlation was found between the number of phases present in a single crystal feldspar (i.e. whether it is single phase or perthitic) and electron trapping centres. Thus, observed differences in electron trap depths and IRPL emissions are influenced by additional factors, not explored in this thesis.

The width of the sub-conduction band-tail states range from 0.2 to 0.8 eV in the samples investigated. This suggests different impacts on charge mobility, and stability of trapped electrons in these samples. The intensity and stability of the blue luminescence emission (~410 nm), the emission most commonly used in luminescence dating studies, is suggested to be influenced by the degree of order of Al³⁺ ions on the framework. It is proposed that crystal defects giving rise to the blue luminescence emission are not only related to feldspars from geological environments where the high structural state (disorder of Al³⁺ ions on the framework) is retained during rapid cooling of the magma (e.g. volcanic

origin), but is also related to perthites. In perthites the interfaces between K- and Na-feldspar lamellae are likely to host a high density of defects, resulting not only in intense blue emission, but also in high anomalous fading rates, making fading correction of luminescence ages inevitable.

Research in this thesis shows the complexity of factors influencing luminescence properties in feldspars, which has to be kept in mind, when trying to further improve the use of feldspars as natural luminescence dosimeters.

Maria Schaarschmidt

Luminescence dating of archaeological and geomorphological sites in central Myanmar and northern Vietnam, Southeast Asia

March 2021

University of Wollongong, Wollongong, NSW, Australia

Degree: Ph.D.

Supervisors: Prof. Richard Roberts, Prof. Bo Li

Southeast Asia plays a key role in understanding the dispersal of early modern humans through South Asia into Australasia. The routes they took are still debated, as is the timing of initial modern human dispersal out of Africa. Multiple scenarios are possible, mainly focussed on Marine Isotope Stages 5 (130–70 ka) through 3 (57–30 ka). During these periods, environmental conditions in Myanmar and Vietnam would have allowed for diverse nutrition strategies and options for shelter. Caves and rock shelters in Myanmar and Vietnam commonly contain evidence of human activity, including stone artefacts and fossil remains. Establishing reliable chronologies for such sites can therefore provide insights into the timing of human occupation and possible routes of hominin dispersal through mainland Southeast Asia.

Archaeological and geomorphological sites may be dated using a variety of geochronological methods. Luminescence dating is potentially applicable to sediments deposited in the last few hundreds of thousands of years, which is the reliable age range for two ubiquitous minerals, quartz and K-feldspar, found in many depositional settings. However, only a few sites in Southeast Asia have been dated using luminescence methods. In this study, four archaeological and geomorphological sites in Myanmar and Vietnam were investigated: Badahlin Cave, Gu Myaung Cave and the Chauk river terraces in central Myanmar, and Nguom rock shelter in northern Vietnam.

Twenty-seven samples were prepared for luminescence dating, using a range of grain-size fractions of quartz and K-feldspar. The optically stimulated luminescence (OSL) signal from individual grains of quartz was measured using a standard single-aliquot regenerative-dose procedure. Single grains of K-feldspar were measured using a two-step post-infrared infrared (pIRIR) procedure, together with a regional standardised growth curve constructed for these samples. The L_nT_n method was used to estimate the equivalent doses for the K-feldspar samples, some of which were

also measured using the infrared radiofluorescence (IR-RF) signal. Environmental dose rates were estimated using beta counting and in situ gamma-ray spectrometry.

The deposits in Badahlin Cave were dated to between ~ 54 and ~ 3 ka, with consistent ages obtained from quartz and K-feldspar for most of the samples. The OSL ages range from ~ 54 ka at the base of the excavation to ~ 5 ka at the top, while the pIRIR ages range from ~ 47 to ~ 3 ka. Systematically and significantly older ages were obtained using the IR-RF signal for dating (~ 87–51 ka), likely due to an undetected and substantial residual dose. At the nearby site of Gu Myaung Cave, the ages range from ~ 19 to ~ 3 ka (OSL) and from ~ 17 to ~ 1 ka (pIRIR). As at Badahlin Cave, the IR-RF ages are significantly older (~ 100–39 ka). The Chauk terraces flanking the Irrawaddy River were dated using OSL and pIRIR methods to between ~ 167 ka, for the uppermost terrace, and ~ 5 ka, for the terrace bordering the river. Samples from the middle terrace produced widely dispersed distributions of equivalent dose comprised of discrete components, with an age of ~ 75–8 ka considered most likely for terrace formation.

The deposits at Nguom rock shelter were dated to between ~ 41 and ~ 11 ka based on the OSL signal, whereas significantly older, maximum age estimates were obtained using the pIRIR signal (~ 187–26 ka). Archaeologically sterile layers in the middle part of the deposit indicate that the cave roof may have collapsed ~ 25 ka, based on the OSL and radiocarbon chronologies.

This study has found that human occupation of Badahlin Cave, Gu Myaung Cave and Nguom rock shelter commenced between ~ 40 and ~ 20 ka, during the late stages of the Pleistocene, and continued through into the Holocene. These findings add to our knowledge of modern human settlement and dispersal through Southeast Asia. The OSL and pIRIR ages obtained for Badahlin and Gu Myaung Caves are the first luminescence ages reported for any site in Myanmar, and excavations at these sites have also yielded the first evidence for bifacial stone artefacts discovered in this part of Southeast Asia. Human occupation of the Chauk terraces seems unlikely at the locations investigated, as no archaeological remains were recovered.

The OSL signal appears to be suitable for dating of Myanmar and Vietnam quartz grains and the pIRIR signal similarly for Myanmar K-feldspars, which presents the opportunity to apply these methods to other sites in the region. IR-RF dating may provide an alternative to OSL and pIRIR methods in the future, but the extent of residual signal and variability in bleaching behaviour require further investigation before reliable IR-RF ages can be obtained.

Atul Kumar Singh

Luminescence Chronology of Late Quaternary Terraces in Darjeeling-Sikkim Himalaya: Implications to Climate and Tectonics

July 2020

Indian Institute of Science Education and Research Kolkata,
Kolkata, India

Degree: Ph.D.

Supervisor: Dr Manoj Kumar Jaiswal

The Himalaya formed due to collision of the Indian and Eurasian plate ~ 50 Ma. Since then it has not been only tectonically active but also has modulated the regional monsoonal precipitation. The Himalaya hold many secrets of past tectonic activities and climate change. This study uses two of geomorphic proxies viz. alluvial fans and fluvial terraces which act as archives preserving information about the past. This study aims at unveiling the past climate changes and tectonic activities during Late Quaternary in Darjeeling-Sikkim Himalaya (DSH).

Alluvial fans are important geomorphic archives because of its strategic location at mountain front. It forms when the sediment supply overwhelms the water discharge and such condition could only be achieved in certain tectonic or climatic setting. We provide a detailed luminescence chronology of Matiali alluvial fan in north West Bengal, India. The regional fan surface (T4) has been dissected by E-W trending Himalayan thrusts known as Matiali and Chalsa thrusts and have various terraces named as T3, T2 and youngest one as T1. Luminescence ages suggest that the formation of the alluvial fan (regional surface) started before 171 ka and continued till 72 ka covering a time span of nearly 100 ky; suggestive of weaker monsoon at 72 ka. Matiali fault activated after 171 ky. Chalsa fault is suggested to be active during 48–41 ka. The last aggradational phase was around 6 ka which led to the formation of T1a terrace. The study suggests that climatic fluctuation during this period were shaping the morphology of the alluvial fan, along with tectonic activities on the two faults.

Further investigation to the south of the Matiali fan reveal the existence of an active fault known as the Baradighi fault. The activity on the Baradighi fault started around 25 ka and it was active in recent past also. The drainage system in the Matiali fan as well as in the Baradighi surface has been highly modified by the tectonics. The Asymmetry factor and Basin elongation ratios also indicated that the river basins in the region are influence by tectonics whereas the Hypsometric Curves and Integral (HI and HC) indicate otherwise. The HI and HC give an idea about the dominance of erosion or tectonics, although the region is tectonically active but is mostly composed of non-lithified Quaternary sediment. Thus, it is easier for the rivers to erode into softer sediments.

Fluvial terraces in the Himalaya are also important geomorphic archives which preserve the signature of tectonics and past environment. Terraces in the DSH fold and thrust

belt have not received much attention of the geologists. An attempt to understand the evolution of paired and deformed terraces between major thrust boundaries of the eastern Himalaya, on the either banks of the Tista River in Darjeeling-Sikkim-Tibet wedge has been made. These terraces are located at the confluence of Tum Thang khola and the Tista River (near Rangpo). Three levels of terraces are present in general and also in the study area. The terrace T3 was formed during last interglacial period and the T2 terrace during last glacial maximum (LGM) and in the humid phases after LGM. The top section of T2 terrace (~ 2.5 m thick) was formed in the transition phase (arid to humid) after Younger Dryas event. The region has experienced several deformational events, (i) one after 45 ka which raised the T3 terrace to its present level, (ii) another one after 11.9 ka which raised the T2 to its present level and this event is also associated with the shifting of the Tum Thang khola, and (iii) the region is still tectonically active as shown by the warping of the T1 and T0 surfaces, which are of recent origin. These terraces have complex input of sediments from Higher Himalayan Crystalline (HHC) rocks and from locally present Lingtse granites. This study was further extended to other sections, viz. Manglay, Sintam and Sevoke for better understanding of the past climatic conditions and neo-tectonics. The study gave similar kind of results and also shows that there was a large-scale change in the gradient of the Tista River after 34 ka.

A PDF of this thesis can be requested by contacting aks-ingh21sep@gmail.com

Giulia Tamburini

Thermally Transferred Optically Stimulated Luminescence (TT-OSL): a dating technique for quartz

March 2021

Dipartimento di Scienza dei Materiali, Università degli Studi di Milano Bicocca, Milano (Italy)

Degree: M. Sc.

Supervisors: Marco Martini, Laura Panzeri

Optically Stimulated Luminescence (OSL) is a very powerful technique that can date samples as old as hundred thousand years or more and its applications cover many areas of Earth sciences for the determination of the age of sediments by measuring how long ago they were last exposed to daylight. In the last few years, the use of a new signal from quartz extracted from sediments has been suggested as a new tool for optical dating. This signal, termed TT-OSL (Thermally Transferred Optically Stimulated Luminescence), originates when the sample is optically bleached and subsequently heated. Two types of transfer contribute to the appearance of this signal: recuperation (Re-OSL) and basic transfer (BT-OSL). The former is due to the presence of electrons in light-insensitive (“hard-to-bleach”) traps prior to the zeroing event and remaining in these traps until the sample is heated; the latter is due to electrons in the OSL traps which,

during the bleaching event, are transferred to light-sensitive traps (“refuge traps”); during preheating, some of these electrons may be transferred back to the OSL traps. TT-OSL signal appears to have the potential to extend by almost an order of magnitude the age range over which OSL luminescence dating can be applied.

This thesis work is devoted to the study of the OSL and TT-OSL signals detected in quartz, both from sediment and as a mineral with different characteristics and provenances. In particular we focused our attention on the factors that may influence its behaviour and on the identification of the traps responsible for this signal studying the TL glow curves. The possibility of effectively using the TT-OSL signal to determine the equivalent dose, in order to apply it to the field of dating will be also discussed.

Firstly the dependence of the TT-OSL signal on the preheating temperature used to induce thermal transfer was studied. It was noticed for all the sample analysed that this signal increases with the temperature until it reaches a peak between 280 and 300 °C, implying that the TT-OSL source trap should correspond to an electron trap with a TL peak at temperatures above 280 °C. Mineral quartz aliquots, specifically rose quartz, show some differences from sedimentary quartz, since the intensities of their OSL and TT-OSL signals are lower by two orders of magnitude. It can be concluded that this behaviour may arise either from sensitisation processes due to repeated cycles of trapping and de-trapping, or from the different nature of the sample, as it has not been subjected to the same heat and light exposures as a sediment. For this purpose, a solar simulator was used in order to increase the intensity of OSL and TT-OSL signals in rose quartz aliquots through the repetition of light exposure and subsequent bleaching cycles of optically-active centres. It was observed that, despite this treatment, the shape of OSL and TT-OSL decay curves remain unchanged, and therefore the different origin of the sample may affect the intensity and behaviour of this signals.

Finally, in order to identify the source traps that contribute to OSL and TT-OSL signals in quartz, variations in Thermoluminescence (TL) glow curves caused by OSL and TT-OSL measurements were studied. By performing comparisons and subtractions between different glow curves, clear optical bleaching effects can be observed. In particular, it is possible to identify the presence of a TT-OSL trap associated with a TL peak at ~ 270 °C, at lower temperatures than that of OSL trap at ~ 280 °C, demonstrating that the two mechanisms have different origins, in agreement with results previously obtained. A PDF of this thesis can be acquired by contacting the author (g.tamburini@campus.unimib.it).

Bibliography

Compiled by Sebastien Huot

From 1st December 2020 to 31st May 2021

Various geological applications

- aeolian

- Durga Prasad, A., Bhattacharya, F., Chauhan, G., Balaji, D., Thakkar, M.G., Rao, Y.S., 2021. Late-Quaternary miliolite (biogenic carbonate) deposits and their implications for sea-level fluctuations and climatic variability. *Earth Surface Processes and Landforms* 46, 921-941, <http://doi.org/10.1002/esp.5067>
- East, A.E., Gray, H.J., Redsteer, M.H., Ballmer, M., 2021. Landscape evolution in eastern Chuckwalla Valley, Riverside County, California, Reston, VA, <http://doi.org/10.3133/sir20215017>
- Han, W., Lü, S., Appel, E., Berger, A., Madsen, D., Vandenberghe, J., Yu, L., Han, Y., Yang, Y., Zhang, T., Teng, X., Fang, X., 2019. Dust storm outbreak in central Asia after ~3.5 kyr BP. *Geophysical Research Letters* 46, 7624-7633, <http://doi.org/10.1029/2018GL081795>
- Robins, L., Greenbaum, N., Yu, L., Bookman, R., Roskin, J., 2021. High-resolution portable-OSL analysis of Vegetated Linear Dune construction in the margins of the northwestern Negev dunefield (Israel) during the late Quaternary. *Aeolian Research* 50, 100680, <http://doi.org/10.1016/j.aeolia.2021.100680>
- Roettig, C.B., Kolb, T., Zöllner, L., Zech, M., Faust, D., 2020. A detailed chrono-stratigraphical record of canarian dune archives - Interplay of sand supply and volcanism. *Journal of Arid Environments* 183, 104240, <http://doi.org/10.1016/j.jaridenv.2020.104240>
- Stolz, C., Suchora, M., Pidek, I.A., Fülling, A., 2021. Lake and inland dunes as interconnected Systems: The story of Lake Tresssee and an adjacent dune field (Schleswig-Holstein, North Germany). *The Holocene* 31, 672-689, <http://doi.org/10.1177/0959683620981684>
- Swezey, C.S., 2020. Quaternary eolian dunes and sand sheets in inland locations of the Atlantic Coastal Plain province, USA, in: Lancaster, N., Hesp, P. (Eds.), *Inland dunes of North America*. Springer International Publishing, Cham, pp. 11-63, http://doi.org/10.1007/978-3-030-40498-7_2
- Xue, H., Zeng, F., 2021. Holocene environmental evolution in the Qinghai Lake area recorded by aeolian deposits. *Quaternary International* 580, 67-77, <http://doi.org/10.1016/j.quaint.2020.12.032>

- alluvial fan

- East, A.E., Gray, H.J., Redsteer, M.H., Ballmer, M., 2021. Landscape evolution in eastern Chuckwalla Valley, Riverside County, California, Reston, VA, <http://doi.org/10.3133/sir20215017>

- cave

- Caldeira, D., Uagoda, R., Nogueira, A.M., Garnier, J., Sawakuchi, A.O., Hussain, Y., 2021. Late Quaternary episodes of clastic sediment deposition in the Tarimba Cave, Central Brazil. *Quaternary International* 580, 22-37, <http://doi.org/10.1016/j.quaint.2021.01.012>
- Karkanias, P., Marean, C., Bar-Matthews, M., Jacobs, Z., Fisher, E., Braun, K., 2021. Cave life histories of non-anthropogenic sediments help us understand associated archaeological contexts. *Quaternary Research* 99, 270-289, <http://doi.org/10.1017/qua.2020.72>
- Mirea, I.-C., Robu, M., Petculescu, A., Keneszi, M., Faur, L., Arghir, R., Tecsa, V., Timar-Gabor, A., Roban, R.-D., Panaiotu, C.G., Sharifi, A., Pourmand, A., Codrea, V.A., Constantin, S., 2021. Last deglaciation flooding events in the Southern Carpathians as revealed by the study of cave deposits from Muierilor Cave, Romania. *Palaeogeography, Palaeoclimatology, Palaeoecology* 562, 110084, <http://doi.org/10.1016/j.palaeo.2020.110084>

- coastal

- Björck, S., Lambeck, K., Möller, P., Waldmann, N., Bennike, O., Jiang, H., Li, D., Sandgren, P., Nielsen, A.B., Porter, C.T., 2021. Relative sea level changes and glacio-isostatic modelling in the Beagle Channel, Tierra del Fuego, Chile: Glacial and tectonic implications. *Quaternary Science Reviews* 251, 106657, <http://doi.org/10.1016/j.quascirev.2020.106657>

- Casini, L., Andreucci, S., Sechi, D., Huang, C.-Y., Shen, C.-C., Pascucci, V., 2020. Luminescence dating of Late Pleistocene faults as evidence of uplift and active tectonics in Sardinia, W Mediterranean. *Terra Nova* 32, 261-271, <http://doi.org/10.1111/ter.12458>
- Collins, D.S., Nguyen, V.L., Ta, T.K.O., Mao, L., Ishii, Y., Kitagawa, H., Nakashima, R., Vo, T.H.Q., Tamura, T., 2021. Sedimentary evolution of a delta-margin mangrove in Can Gio, northeastern Mekong River delta, Vietnam. *Marine Geology* 433, 106417, <http://doi.org/10.1016/j.margeo.2020.106417>
- de Oliveira e Silva, R.C., de Macedo Dias, G.T., 2020. Submerged Pleistocene spodic horizon remnant exposed on the inner continental shelf off Guanabara Bay (Rio de Janeiro, Brazil). *Geo-Marine Letters* 40, 925-933, <http://doi.org/10.1007/s00367-019-00622-x>
- del Valle, L., Fornós, J.J., Pomar, F., Pons, G.X., Timar-Gabor, A., 2020. Aeolian-alluvial interactions at Formentera (Balearic Islands, Western Mediterranean): The late Pleistocene evolution of a costal system. *Quaternary International* 566-567, 271-283, <http://doi.org/10.1016/j.quaint.2020.05.010>
- Durga Prasad, A., Bhattacharya, F., Chauhan, G., Balaji, D., Thakkar, M.G., Rao, Y.S., 2021. Late-Quaternary miliolite (biogenic carbonate) deposits and their implications for sea-level fluctuations and climatic variability. *Earth Surface Processes and Landforms* 46, 921-941, <http://doi.org/10.1002/esp.5067>
- Ferranti, L., Burrato, P., Sechi, D., Andreucci, S., Pepe, F., Pascucci, V., 2021. Late Quaternary coastal uplift of southwestern Sicily, central Mediterranean sea. *Quaternary Science Reviews* 255, 106812, <http://doi.org/10.1016/j.quascirev.2021.106812>
- Fruergaard, M., Sander, L., Goslin, J., Andersen, T.J., 2021. Temporary late Holocene barrier-chain deterioration due to insufficient sediment availability, Wadden Sea, Denmark. *Geology* 49, 162-167, <http://doi.org/10.1130/G47978.1>
- Gao, L., Long, H., Tamura, T., Hou, Y., Shen, J., 2021. A ~130 ka terrestrial-marine interaction sedimentary history of the northern Jiangsu coastal plain in China. *Marine Geology* 435, 106455, <http://doi.org/10.1016/j.margeo.2021.106455>
- Han, M., Kim, J.C., Yang, D.Y., Lim, J., Yi, S., 2021. The main periods and environmental controls of coastal dune development along the west coast of the Korean Peninsula during the mid to late Holocene. *Palaeogeography, Palaeoclimatology, Palaeoecology* 569, 110345, <http://doi.org/10.1016/j.palaeo.2021.110345>
- Lampe, R., Lampe, M., 2021. The role of sea-level changes in the evolution of coastal barriers – An example from the southwestern Baltic Sea. *The Holocene* 31, 515-528, <http://doi.org/10.1177/0959683620981703>
- McBride, R.A., Oliver, T.S.N., Dougherty, A.J., Tamura, T., Carvalho, R.C., Short, A.D., Woodroffe, C.D., 2021. The turnaround from transgression to regression of Holocene barrier systems in south-eastern Australia: Geomorphology, geological framework and geochronology. *Sedimentology* 68, 943-986, <http://doi.org/10.1111/sed.12812>
- Morthekai, P., Nageswara Rao, K., Nagakumar, K.C.V., Demudu, G., Rajapara, H.M., Reddy, D.V., 2021. Synthesized luminescence ages of palaeo-beach ridges in Krishna–Godavari twin delta plain, east coast of India. *Quaternary Geochronology* 62, 101145, <http://doi.org/10.1016/j.quageo.2020.101145>
- Nian, X., Zhang, W., Wang, Z., Sun, Q., Chen, Z., 2021. Inter-comparison of optically stimulated luminescence (OSL) ages between different fractions of Holocene deposits from the Yangtze delta and its environmental implications. *Marine Geology* 432, 106401, <http://doi.org/10.1016/j.margeo.2020.106401>
- Özpolat, E., Şahiner, E., Özcan, O., Demir, T., Owen, L.A., 2021. Late-Holocene landscape evolution of a delta from foredune ridges: Seyhan Delta, Eastern Mediterranean, Turkey. *The Holocene* 31, 760-777, <http://doi.org/10.1177/0959683620988047>
- Panario, D., Bracco Boksar, R., Gutiérrez, O., Tassano, M., 2019. OSL Dating of Lagoon Geofoms as Proxies of Marine Levels for the Late Holocene, in: Inda Ferrero, H., García Rodríguez, F. (Eds.), *Advances in Coastal Geoarchaeology in Latin America*. Springer International Publishing, Cham, pp. 35-48, http://doi.org/10.1007/978-3-030-17828-4_3
- Sainz de Murieta, E., Cunha, P.P., Cearreta, A., Murray, A.S., Buylaert, J.-P., 2021. The Oyambre coastal terrace: a detailed sedimentary record of the Last Interglacial Stage in northern Iberia (Cantabrian coast, Spain). *Journal of Quaternary Science* 36, 570-585, <http://doi.org/10.1002/jqs.3317>
- Shu, Q., Zhao, Y., Frechen, M., Zhang, J., Chen, Y., Liu, Y., Yang, P., 2021a. Chronology of a sedimentary sequence from the land–ocean interaction zone in the North Jiangsu Basin. *Quaternary International* 580, 78-86, <http://doi.org/10.1016/j.quaint.2020.11.029>
- Shu, Q., Zhao, Y., Hu, Z., Yang, P., Liu, Y., Chen, Y., Zhao, Z., Zhang, M., 2021b. Multi-proxy reconstruction of the Holocene transition from a transgressive to regressive coastal evolution in the northern Jiangsu Plain, East China. *Palaeogeography, Palaeoclimatology, Palaeoecology* 572, 110405, <http://doi.org/10.1016/j.palaeo.2021.110405>

- Softa, M., Spencer, J.Q.G., Sözbülür, H., Huot, S., Emre, T., 2021. Luminescence dating of Quaternary marine terraces from the coastal part of Eastern Black Sea and their tectonic implications for the Eastern Pontides, Turkey. *Turkish Journal of Earth Sciences* 30, 359-378, <http://doi.org/10.3906/yer-2005-21>
- Torres, J., Kulp, M., FitzGerald, D., Georgiou, I., Lepper, K., 2020. Geomorphic and temporal evolution of a Mississippi delta flanking barrier island: Grand Isle, LA. *Marine Geology* 430, 106341, <http://doi.org/10.1016/j.margeo.2020.106341>
- Uścińowicz, S., Adamiec, G., Bluszcz, A., Jegliński, W., Miotk-Szpiganowicz, G., 2021. Holocene development of the Vistula Spit (Baltic Sea coast) based on multidisciplinary investigations. *The Holocene* 31, 658-671, <http://doi.org/10.1177/0959683620983410>

- colluvial

- Corrêa, A.C.D.B., Monteiro, K.D.A., 2020. Geomorphological dynamics of the elevated geosystems of the Borborema highlands, northeast of Brazil, from optically stimulated luminescence dating of hillslope sediments William Morris Davis - *Revista de Geomorfologia* 1, 162-185, <https://williammorrisdavis.uvanet.br/index.php/revistageomorfologia/article/view/32>
- Scherer, S., Deckers, K., Dietel, J., Fuchs, M., Henkner, J., Höpfer, B., Junge, A., Kandeler, E., Lehndorff, E., Leinweber, P., Lomax, J., Miera, J., Poll, C., Toffolo, M.B., Knopf, T., Scholten, T., Kühn, P., 2021. What's in a colluvial deposit? Perspectives from archaeopedology. *CATENA* 198, 105040, <http://doi.org/10.1016/j.catena.2020.105040>
- Wang, L., Yang, Z., Liu, G., Liu, S., Fu, X., Qiao, J., 2021. Dynamic processes of the Dora Kamiyama rockslide in the Tibetan Plateau, China: geomorphic implication. *Bulletin of Engineering Geology and the Environment* 80, 933-950, <http://doi.org/10.1007/s10064-020-02004-5>

- earthquake (and fault related)

- Cao, X., Hu, X., Pan, B., Zhao, Q., Chen, T.a., Ji, X., Zhao, Z., 2021. Using fluvial terraces as distributed deformation offset markers: Implications for deformation kinematics of the North Qilian Shan Fault. *Geomorphology* 386, 107750, <http://doi.org/10.1016/j.geomorph.2021.107750>
- De Masi, C., Koehler, R., Dee, S., Keen-Zebert, A., 2021. Early development of strike-slip faulting: palaeoseismic study along the Petersen Mountain fault, northern Walker Lane, Nevada. *Journal of Quaternary Science* 36, 403-414, <http://doi.org/10.1002/jqs.3283>
- Duman, T.Y., Elmacı, H., Özalp, S., Kürçer, A., Kara, M., Özdemir, E., Yavuzoğlu, A., Uygün Gülüdoğan, Ç., 2020. Paleoseismology of the western Sürgü-Misis fault system: East Anatolian Fault, Turkey. *Mediterranean Geoscience Reviews* 2, 411-437, <http://doi.org/10.1007/s42990-020-00041-6>
- DuRoss, C.B., Gold, R.D., Briggs, R.W., Delano, J.E., Ostenaar, D.A., Zellman, M.S., Cholewinski, N., Wittke, S.J., Mahan, S.A., 2020. Holocene earthquake history and slip rate of the southern Teton fault, Wyoming, USA. *GSA Bulletin* 132, 1566-1586, <http://doi.org/10.1130/B35363.1>
- Moraetis, D., Scharf, A., Mattern, F., Pavlopoulos, K., Forman, S., 2020. Quaternary thrusting in the Central Oman Mountains—novel observations and causes: Insights from optical stimulate luminescence dating and kinematic fault analyses. *Geosciences* 10, 166, <https://www.mdpi.com/2076-3263/10/5/166>
- Nelson, A.R., DuRoss, C.B., Witter, R.C., Kelsey, H.M., Engelhart, S.E., Mahan, S.A., Gray, H.J., Hawkes, A.D., Horton, B.P., Padgett, J.S., 2021. A maximum rupture model for the central and southern Cascadia subduction zone—reassessing ages for coastal evidence of megathrust earthquakes and tsunamis. *Quaternary Science Reviews* 261, 106922, <http://doi.org/10.1016/j.quascirev.2021.106922>
- Rajendran, C.P., 2021. Constraints on previous earthquakes from the liquefaction sites in the Kathmandu Valley associated with the 2015 Gorkha earthquake and their regional implications. *Quaternary International* 585, 44-54, <http://doi.org/10.1016/j.quaint.2020.10.053>
- Thomas, F., Rizza, M., Bellier, O., Billant, J., Dussouillez, P., Fleury, J., Delanghe, D., Ollivier, V., Godard, V., Talon, B., 2021. Assessing post-pliocene deformation in a context of slow tectonic deformation: insights from paleoseismology, remote sensing and shallow geophysics in Provence, France. *Natural Hazards* 105, 1453-1490, <http://doi.org/10.1007/s11069-020-04362-5>
- Tsoni, M., Iliopoulos, G., Valavani, D., Liapi, E., Papadopoulou, P., Stamoulis, K., Koukouvelas, I., Kontopoulou, N., 2021. Palaeoenvironmental inferences on the Pleistocene deposits of the Charadros River (Rio graben, Western Corinth Gulf, Greece). *Quaternary International* 589, 39-54, <http://doi.org/10.1016/j.quaint.2021.03.036>
- Zellman, M.S., DuRoss, C.B., Thackray, G.D., Personius, S.F., Reitman, N.G., Mahan, S.A., Brossy, C.C., 2020. Holocene Rupture History of the Central Teton Fault at Leigh Lake, Grand Teton National Park, Wyoming. *Bulletin of the Seismological Society of America* 110, 67-82, <http://doi.org/10.1785/0120190129>

- fluvial

- Bahain, J.-J., Voinchet, P., Vietti, A., Shao, Q., Tombret, O., Pereira, A., Nomade, S., Falguères, C., 2021. ESR/U-series and ESR dating of several Middle Pleistocene Italian sites: Comparison with ⁴⁰Ar/³⁹Ar chronology. *Quaternary Geochronology* 63, 101151, <http://doi.org/10.1016/j.quageo.2021.101151>
- Bender, A.M., Lease, R.O., Corbett, L.B., Bierman, P.R., Caffee, M.W., Rittenour, T.M., 2020. Late Cenozoic climate change paces landscape adjustments to Yukon River capture. *Nature Geoscience* 13, 571-575, <http://doi.org/10.1038/s41561-020-0611-4>
- Brown, A.G., Rhodes, E.J., Davis, S., Zhang, Y., Pears, B., Whitehouse, N.J., Bradley, C., Bennett, J., Schwenninger, J.-L., Firth, A., Firth, E., Hughes, P., Walling, D., 2021. Late Quaternary evolution of a lowland anastomosing river system: Geological-topographic inheritance, non-uniformity and implications for biodiversity and management. *Quaternary Science Reviews* 260, 106929, <http://doi.org/10.1016/j.quascirev.2021.106929>
- Chahal, P., Kumar, A., Sharma, P.C., Sundriyal, Y.P., Srivastava, P., 2020. A preliminary assessment of the geological evidence of the mega floods in the upper Zaskar catchment, NW Himalaya. *Journal of The Palaeontological Society of India* 65, 64-72, https://palaeontologicalsociety.in/vol65_June/6.%20Poonam_et_al_MS-reformat-old.pdf
- Chatterjee, A., Ray, J.S., Shukla, A.D., Pande, K., 2019. On the existence of a perennial river in the Harappan heartland. *Scientific Reports* 9, 17221, <http://doi.org/10.1038/s41598-019-53489-4>
- East, A.E., Gray, H.J., Redsteer, M.H., Ballmer, M., 2021. Landscape evolution in eastern Chuckwalla Valley, Riverside County, California, Reston, VA, <http://doi.org/10.3133/sir20215017>
- Elznicová, J., Kiss, T., Sipos, G., Faměra, M., Štojdil, J., Váchová, V., Matys Grygar, T., 2021. A central European alluvial river under anthropogenic pressure: The Ohře River, Czechia. *CATENA* 201, 105218, <http://doi.org/10.1016/j.catena.2021.105218>
- Guzmán, O., Díaz, M., Campos, C., González, A., Vassallo, R., Aranda, N., Conicelli, B., González-Laprea, J., 2021. First ESR dating of quaternary sediments in Mérida Andes, Western Venezuela. *Journal of South American Earth Sciences* 106, 103089, <http://doi.org/10.1016/j.jsames.2020.103089>
- Ishii, Y., Tamura, T., Ben, B., 2021. Holocene sedimentary evolution of the Mekong River floodplain, Cambodia. *Quaternary Science Reviews* 253, 106767, <http://doi.org/10.1016/j.quascirev.2020.106767>
- Kurbanov, R., Murray, A., Thompson, W., Svistunov, M., Taratunina, N., Yanina, T., 2021. First reliable chronology for the Early Khvalynian Caspian Sea transgression in the Lower Volga River valley. *Boreas* 50, 134-146, <http://doi.org/10.1111/bor.12478>
- Li, J., Yuan, S., Liu, Y., Liu, X., Bai, X., Jiang, J., Li, Y., Zhao, Z., 2019. Tectonic Uplift of the Yili Basin during the Last Stage of the Late Pleistocene: Evidence from ESR and OSL Dating of Sediments in the Huocheng Area, Xinjiang. *Acta Geologica Sinica - English Edition* 93, 1219-1227, <http://doi.org/10.1111/1755-6724.14355>
- McClain, K.P., Yıldırım, C., Çiner, A., Sarıkaya, M.A., Özcan, O., Görüm, T., Köse, O., Şahin, S., Kıyak, N.G., Öztürk, T., 2021. River, alluvial fan and landslide interactions in a tributary junction setting: Implications for tectonic controls on Quaternary fluvial landscape development (Central Anatolian Plateau northern margin, Turkey). *Geomorphology* 376, 107567, <http://doi.org/10.1016/j.geomorph.2020.107567>
- Purtill, M.P., Kite, J.S., Forman, S.L., 2019. Geochronology and depositional history of the sandy springs aeolian landscape in the unglaciated upper Ohio River valley, United States. *Frontiers in Earth Science* 7, <http://doi.org/10.3389/feart.2019.00322>
- Scott, L., Manzano, S., Carr, A.S., Cordova, C., Ochando, J., Bateman, M.D., Carrión, J.S., 2021. A 14000 year multi-proxy alluvial record of ecotone changes in a Fynbos-Succulent Karoo transition in South Africa. *Palaeogeography, Palaeoclimatology, Palaeoecology* 569, 110331, <http://doi.org/10.1016/j.palaeo.2021.110331>
- Shen, Z., Rosenheim, B.E., Törnqvist, T.E., Lang, A., 2021. Engineered continental-scale rivers can drive changes in the carbon cycle. *AGU Advances* 2, e2020AV000273, <http://doi.org/10.1029/2020AV000273>
- Singh, A., Jain, V., Danino, M., Chauhan, N., Kaushal, R.K., Guha, S., Prabhakar, V.N., 2021. Larger floods of Himalayan foothill rivers sustained flows in the Ghaggar–Hakra channel during Harappan age. *Journal of Quaternary Science* 36, 611-627, <http://doi.org/10.1002/jqs.3320>
- Solanki, T., Prizomwala, S.P., Makwana, N., Solanki, P.M., 2021. Assessing the climatically triggered aggradation-incision processes in a dryland environment during the Late Quaternary period from Shetrunji River basin (Saurashtra), India. *Quaternary International* 585, 70-84, <http://doi.org/10.1016/j.quaint.2020.07.007>
- Thamó-Bozsó, E., Csillag, G., Fűri, J., Nagy, A., Magyari, Á., 2020. Age of sediments on Danube terraces of the Pest Plain (Hungary) based on optically stimulated luminescence dating of quartz and feldspar. *Geochronometria* 47, 171-186, <http://doi.org/10.2478/geochr-2020-0021>

- Tian, Q., Kirby, E., Zheng, W., Zhang, H., Liang, H., Li, Z., Wang, W., Li, T., Zhang, Y., Xu, B., Zhang, P., 2021. Late Quaternary variations in paleoerosion rates in the northern Qilian Shan revealed by ¹⁰Be in fluvial terraces. *Geomorphology* 386, 107751, <http://doi.org/10.1016/j.geomorph.2021.107751>
- Wang, B., Wang, X., Yi, S., Zhao, L., Lu, H., 2021a. Responses of fluvial terrace formation to monsoon climate changes in the north-eastern Tibetan Plateau: Evidence from pollen and sedimentary records. *Palaeogeography, Palaeoclimatology, Palaeoecology* 564, 110196, <http://doi.org/10.1016/j.palaeo.2020.110196>
- Wang, H., Huang, C.C., Pang, J., Zhou, Y., Cuan, Y., Guo, Y., Zhang, Y., Zhou, Q., Rong, X., Shang, R., 2021b. Catastrophic flashflood and mudflow events in the pre-historical Lajia Ruins at the northeast margin of the Chinese Tibetan Plateau. *Quaternary Science Reviews* 251, 106737, <http://doi.org/10.1016/j.quascirev.2020.106737>
- Wasson, R.J., Ziegler, A., Lim, H.S., Teo, E., Lam, D., Higgitt, D., Rittenour, T., Ramdzan, K.N.B.M., Joon, C.C., Singhvi, A.K., 2021. Episodically volatile high energy non-cohesive river-floodplain systems: New information from the Ping River, Thailand, and a global review. *Geomorphology* 382, 107658, <http://doi.org/10.1016/j.geomorph.2021.107658>
- Zhang, J., Yang, H., Liu-Zeng, J., Ge, Y., Wang, W., Yao, W., Xu, S., 2021. Reconstructing the incision of the Lancang River (Upper Mekong) in southeastern Tibet below its prominent knickzone using fluvial terraces and transient tributary profiles. *Geomorphology* 376, 107551, <http://doi.org/10.1016/j.geomorph.2020.107551>
- Zhou, L., Shi, Y., Zhao, Y., Yang, Y., Jia, J., Gao, J., Wang, Y.P., Li, Z., Zhang, Y., Guo, Y., Shi, B., Gao, S., 2021. Extreme floods of the Changjiang River over the past two millennia: Contributions of climate change and human activity. *Marine Geology* 433, 106418, <http://doi.org/10.1016/j.margeo.2020.106418>

- glacial and periglacial

- Benito, G., Thorndycraft, V.R., Medialdea, A., Machado, M.J., Sancho, C., Dussailant, A., 2021. Declining discharge of glacier outburst floods through the Holocene in central Patagonia. *Quaternary Science Reviews* 256, 106810, <http://doi.org/10.1016/j.quascirev.2021.106810>
- Björck, S., Lambeck, K., Möller, P., Waldmann, N., Bennike, O., Jiang, H., Li, D., Sandgren, P., Nielsen, A.B., Porter, C.T., 2021. Relative sea level changes and glacio-isostatic modelling in the Beagle Channel, Tierra del Fuego, Chile: Glacial and tectonic implications. *Quaternary Science Reviews* 251, 106657, <http://doi.org/10.1016/j.quascirev.2020.106657>
- Buckland, P.I., Bateman, M.D., Bennike, O., Buckland, P.C., Chase, B.M., Frederick, C., Greenwood, M., Murton, J., Murton, D., Panagiotakopulu, E., 2019. Mid-Devensian climate and landscape in England: new data from Finningley, South Yorkshire. *Royal Society Open Science* 6, 190577, <http://doi.org/10.1098/rsos.190577>
- Christ, A.J., Bierman, P.R., Schaefer, J.M., Dahl-Jensen, D., Steffensen, J.P., Corbett, L.B., Peteet, D.M., Thomas, E.K., Steig, E.J., Rittenour, T.M., Tison, J.-L., Blard, P.-H., Perdrial, N., Dethier, D.P., Lini, A., Hidy, A.J., Caffee, M.W., Southon, J., 2021. A multimillion-year-old record of Greenland vegetation and glacial history preserved in sediment beneath 1.4 km of ice at Camp Century. *Proceedings of the National Academy of Sciences* 118, e2021442118, <http://doi.org/10.1073/pnas.2021442118>
- Curry, B.B., Kehew, A.E., Antinao, J.L., Esch, J., Huot, S., Caron, O.J., Thomason, J.F., 2021. Deglacial Kankakee Torrent, source to sink, 548. in: Waitt, R.B., Thackray, G.D., Gillespie, A.R. (Eds.), *Untangling the Quaternary Period—A Legacy of Stephen C. Porter*. Geological Society of America, pp. 317-332, [http://doi.org/10.1130/2020.2548\(16\)](http://doi.org/10.1130/2020.2548(16))
- García, J.-L., Lüthgens, C., Vega, R.M., Rodés, Á., Hein, A.S., Binnie, S.A., 2021. A composite ¹⁰Be, IR-50 and ¹⁴C chronology of the pre-Last Glacial Maximum (LGM) full ice extent of the western Patagonian Ice Sheet on the Isla de Chiloé, south Chile (42° S). *E&G Quaternary Science Journal* 70, 105-128, <http://doi.org/10.5194/egqsj-70-105-2021>
- He, R., Jin, H., French, H.M., Vandenberghe, J., Li, X., Li, F., Jiang, G., Zhang, Z., Chen, X., Serban, R.D., Wang, S., Guo, D., 2021. Cryogenic wedges and cryoturbations on the Ordos Plateau in North China since 50 ka BP and their paleoenvironmental implications. *Permafrost and Periglacial Processes* 32, 231-247, <http://doi.org/10.1002/ppp.2084>
- Kalińska, E., Alexanderson, H., Krievāns, M., 2020. The Raunis section, central Latvia, revisited: first luminescence results and re-evaluation of a key Baltic States stratigraphic site. *Geografiska Annaler: Series A, Physical Geography* 102, 376-396, <http://doi.org/10.1080/04353676.2020.1813982>
- Mleczak, M., Pisarska-Jamroży, M., 2021. A record of deglaciation-related shifting of the proximal zone of a sandur — a case study from the Gwda sandur, NW Poland (MIS 2). *Journal of Palaeogeography* 10, 12, <http://doi.org/10.1186/s42501-021-00089-x>

- Moska, P., Jary, Z., Sokołowski, R.J., Poręba, G., Raczyk, J., Krawczyk, M., Skurzyński, J., Zieliński, P., Michczyński, A., Tudyka, K., Adamiec, G., Piotrowska, N., Pawełczyk, F., Łopuch, M., Szymak, A., Ryzner, K., 2020. Chronostratigraphy of Late Glacial aeolian activity in SW Poland – A case study from the Niemodlin Plateau. *Geochronometria* 47, 124-137, <http://doi.org/10.2478/geochr-2020-0015>
- Nawaz Ali, S., Morthekai, P., Bajpai, S., Phartiyal, B., Sharma, A., Firoze Quamar, M., Prizomwala, S., 2019. Redefining the timing of Tongul glacial stage in the Suru valley, NW Himalaya, India: New insights from luminescence dating. *Journal of Earth System Science* 129, 16, <http://doi.org/10.1007/s12040-019-1280-9>
- Palstra, S.W.L., Wallinga, J., Viveen, W., Schoorl, J.M., van den Berg, M., van der Plicht, J., 2021. Cross-comparison of last glacial radiocarbon and OSL ages using periglacial fan deposits. *Quaternary Geochronology* 61, 101128, <http://doi.org/10.1016/j.quageo.2020.101128>
- Teller, J.T., Owen, L.A., 2021. Age of Gimli beach of Lake Agassiz based on new OSL dating. *Journal of Quaternary Science* 36, 56-65, <http://doi.org/10.1002/jqs.3257>
- Young, R.A., Gordon, L.M., Owen, L.A., Huot, S., Zervas, T.D., 2020. Evidence for a late glacial advance near the beginning of the Younger Dryas in western New York State: An event postdating the record for local Laurentide ice sheet recession. *Geosphere* 17, 271-305, <http://doi.org/10.1130/GES02257.1>

- lacustrine

- East, A.E., Gray, H.J., Redsteer, M.H., Ballmer, M., 2021. Landscape evolution in eastern Chuckwalla Valley, Riverside County, California, Reston, VA, <http://doi.org/10.3133/sir20215017>
- Forbes, M., Cohen, T., Jacobs, Z., Marx, S., Barber, E., Dodson, J., Zamora, A., Cadd, H., Francke, A., Constantine, M., Mooney, S., Short, J., Tibby, J., Parker, A., Cendón, D., Peterson, M., Tyler, J., Swallow, E., Haines, H., Gadd, P., Woodward, C., 2021. Comparing interglacials in eastern Australia: A multi-proxy investigation of a new sedimentary record. *Quaternary Science Reviews* 252, 106750, <http://doi.org/10.1016/j.quascirev.2020.106750>
- Hou, Y., Long, H., Shen, J., Gao, L., 2021. Holocene lake-level fluctuations of Selin Co on the central Tibetan plateau: Regulated by monsoonal precipitation or meltwater? *Quaternary Science Reviews* 261, 106919, <http://doi.org/10.1016/j.quascirev.2021.106919>
- Lisé-Pronovost, A., Fletcher, M.-S., Simon, Q., Jacobs, Z., Gadd, P.S., Heslop, D., Herries, A.I.R., Yokoyama, Y., team, A., 2021. Chronostratigraphy of a 270-ka sediment record from Lake Selina, Tasmania: Combining radiometric, geomagnetic and climatic dating. *Quaternary Geochronology* 62, 101152, <http://doi.org/10.1016/j.quageo.2021.101152>
- Mujtaba, S.A.I., Lal, R., Saini, H.S., Kumar, P., Pant, N.C., 2018. Formation and breaching of two palaeolakes around Leh, Indus valley, during the late Quaternary. *Geological Society, London, Special Publications* 462, 23-34, <http://doi.org/10.1144/sp462.3>
- Orhan, H., Delikan, A., Demir, A., Kapan, S., Olgun, K., Özmen, A., Sayın, Ü., Ekici, G., Aydın, H., Engin, B., Tapramaz, R., 2021. Late Quaternary paleoclimatic and paleoenvironmental changes in the Konya Closed Basin (Konya, Turkey) recorded by geochemical proxies from lacustrine sediments. *Arabian Journal of Geosciences* 14, 766, <http://doi.org/10.1007/s12517-021-07030-5>
- Reheis, M.C., Caskey, J., Bright, J., Paces, J.B., Mahan, S., Wan, E., 2020. Pleistocene lakes and paleohydrologic environments of the Tecopa basin, California: Constraints on the drainage integration of the Amargosa River. *GSA Bulletin* 132, 1537-1565, <http://doi.org/10.1130/B35282.1>
- Zhao, Y., Tzedakis, P.C., Li, Q., Qin, F., Cui, Q., Liang, C., Birks, H.J.B., Liu, Y., Zhang, Z., Ge, J., Zhao, H., Felde, V.A., Deng, C., Cai, M., Li, H., Ren, W., Wei, H., Yang, H., Zhang, J., Yu, Z., Guo, Z., 2020. Evolution of vegetation and climate variability on the Tibetan Plateau over the past 1.74 million years. *Science Advances* 6, eaay6193, <http://doi.org/10.1126/sciadv.aay6193>
- Zhen, Z., Li, W., Xu, L., Zhang, X., Zhang, J., 2021. Lake-level variation of Dali Lake in mid-east of inner Mongolia since the Late Holocene. *Quaternary International* 583, 62-69, <http://doi.org/10.1016/j.quaint.2021.03.003>

- loess

- Bradák, B., Csonka, D., Novothny, Á., Szeberényi, J., Medved'ová, A., Rostinsky, P., Fehér, K., Barta, G., Végh, T., Kiss, K., Megyeri, M., 2021. Late Pleistocene paleosol formation in a dynamic aggradational microenvironment - A case study from the Malá nad Hronom loess succession (Slovakia). *CATENA* 199, 105087, <http://doi.org/10.1016/j.catena.2020.105087>
- Brezeanu, D., Avram, A., Micallef, A., Cinta Pinzaru, S., Timar-Gabor, A., 2021. Investigations on the luminescence properties of quartz and feldspars extracted from loess in the Canterbury Plains, New Zealand South Island. *Geochronometria* 48, 46-60, <http://doi.org/10.2478/geochr-2021-0005>

- D'Amico, M.E., Casati, E., Andreucci, S., Martini, M., Panzeri, L., Sechi, D., El Khair, D.A., Previtali, F., 2021. New dates of a Northern Italian loess deposit (Monte Orfano, Southern pre-Alps, Brescia). *Journal of Soils and Sediments* 21, 832-841, <http://doi.org/10.1007/s11368-020-02860-4>
- Ge, B., Liu, A., 2017. Optically stimulated luminescence dating and analysis of environmentally sensitive grain-size component of Loess in the northern slope of Tianshan Mountains. *Journal of Arid Land Resources and Environment*, 110-116, <http://caod.oriprobe.com/order.htm?id=49675306&ftext=base>
- Jia, J., Chen, J., Wang, Z., Chen, S., Wang, Q., Wang, L., Yang, L., Xia, D., Chen, F., 2021. No evidence for an anti-phased Holocene moisture regime in mountains and basins in Central Asian: Records from Ili loess, Xinjiang. *Palaeogeography, Palaeoclimatology, Palaeoecology* 572, 110407, <http://doi.org/10.1016/j.palaeo.2021.110407>
- Kang, S., Du, J., Wang, N., Dong, J., Wang, D., Wang, X., Qiang, X., Song, Y., 2020. Early Holocene weakening and mid- to late Holocene strengthening of the East Asian winter monsoon. *Geology* 48, 1043-1047, <http://doi.org/10.1130/G47621.1>
- Kehl, M., Vlamincx, S., Köhler, T., Laag, C., Rolf, C., Tsukamoto, S., Frechen, M., Sumita, M., Schmincke, H.-U., Khormali, F., 2021. Pleistocene dynamics of dust accumulation and soil formation in the southern Caspian Lowlands - New insights from the loess-paleosol sequence at Neka-Abelou, northern Iran. *Quaternary Science Reviews* 253, 106774, <http://doi.org/10.1016/j.quascirev.2020.106774>
- Kong, F., Xu, S., Han, M., Chen, H., Miao, X., Kong, X., Jia, G., 2021. Application of grain size endmember analysis in the study of dust accumulation processes: A case study of loess in Shandong Province, East China. *Sedimentary Geology* 416, 105868, <http://doi.org/10.1016/j.sedgeo.2021.105868>
- Lanczont, M., Poltowicz-Bobak, M., Bobak, D., Mroczek, P., Nowak, A., Komar, M., Stanzikowski, K., 2021. On the edge of eastern and western culture zones in the early Late Pleistocene. Świąte 9 – A new epigravettian site in the south-east of Poland. *Quaternary International* 587-588, 172-188, <http://doi.org/10.1016/j.quaint.2020.08.028>
- Mazneva, E., Konstantinov, E., Zakharov, A., Sychev, N., Tkach, N., Kurbanov, R., Sedaeva, K., Murray, A., 2021. Middle and Late Pleistocene loess of the Western Ciscaucasia: Stratigraphy, lithology and composition. *Quaternary International* 590, 146-163, <http://doi.org/10.1016/j.quaint.2020.11.039>
- Scheidt, S., Berg, S., Hambach, U., Klasen, N., Pötter, S., Stolz, A., Veres, D., Zeeden, C., Brill, D., Brückner, H., Kusch, S., Laag, C., Lehmkuhl, F., Melles, M., Monnens, F., Oppermann, L., Rethemeyer, J., Nett, J.J., 2021. Chronological assessment of the Balta Alba Kurgan loess-paleosol section (Romania) – a comparative study on different dating methods for a robust and precise age model. *Frontiers in Earth Science* 8, <http://doi.org/10.3389/feart.2020.598448>
- Wang, H., Huang, C.C., Pang, J., Zhou, Y., Cuan, Y., Guo, Y., Zhang, Y., Zhou, Q., Rong, X., Shang, R., 2021a. Catastrophic flashflood and mudflow events in the pre-historical Lajia Ruins at the northeast margin of the Chinese Tibetan Plateau. *Quaternary Science Reviews* 251, 106737, <http://doi.org/10.1016/j.quascirev.2020.106737>
- Wang, X., Peng, J., Adamiec, G., 2021b. Extending the age limit of quartz OSL dating of Chinese loess using a new multiple-aliquot regenerative-dose (MAR) protocol with carefully selected preheat conditions. *Quaternary Geochronology* 62, 101144, <http://doi.org/10.1016/j.quageo.2020.101144>
- Wei, H., Wang, L., Azarmdel, H., Khormali, F., Frechen, M., Li, G., Chen, F., 2021. Quartz OSL dating of loess deposits since the late glacial in the Southeast of Caspian Sea. *Quaternary International* 583, 39-47, <http://doi.org/10.1016/j.quaint.2020.04.042>
- Wu, P., Xie, Y., Chi, Y., Kang, C., Sun, L., Wei, Z., Zhang, M., Zhang, Y., 2021. Loess accumulation in Harbin with implications for late Quaternary aridification in the Songnen Plain, Northeast China. *Palaeogeography, Palaeoclimatology, Palaeoecology* 570, 110365, <http://doi.org/10.1016/j.palaeo.2021.110365>
- Yang, S., Liu, N., Li, D., Cheng, T., Liu, W., Li, S., Chen, H., Liu, L., Luo, Y., 2021. Quartz OSL chronology of the loess deposits in the Western Qinling Mountains, China, and their palaeoenvironmental implications since the Last Glacial period. *Boreas* 50, 294-307, <http://doi.org/10.1111/bor.12473>
- soil**
- Meyer, N., Kuhwald, M., Petersen, J.F., Duttman, R., 2021. Soil development in weathering pits of a granitic dome (Enchanted Rock) in central Texas. *CATENA* 199, 105084, <http://doi.org/10.1016/j.catena.2020.105084>
- Wallinga, J., Sevink, J., van Mourik, J.M., Reimann, T., 2019. Chapter 4 - Luminescence dating of soil archives, 18. in: Van Mourik, J.M., Van Der Meer, J.J.M. (Eds.), *Reading the Soil Archives: Unraveling the geoecological code of palaeosols and sediment cores*. Elsevier, pp. 115-162, <http://doi.org/10.1016/B978-0-444-64108-3.00004-5>

Wang, H., Huang, C.C., Pang, J., Zhou, Y., Cuan, Y., Guo, Y., Zhang, Y., Zhou, Q., Rong, X., Shang, R., 2021. Catastrophic flashflood and mudflow events in the pre-historical Lajia Ruins at the northeast margin of the Chinese Tibetan Plateau. *Quaternary Science Reviews* 251, 106737, <http://doi.org/10.1016/j.quascirev.2020.106737>

- surface exposure dating

Elkadi, J., King, G.E., Lehmann, B., Herman, F., 2021. Reducing variability in OSL rock surface dating profiles. *Quaternary Geochronology* 64, 101169, <http://doi.org/10.1016/j.quageo.2021.101169>

Galli, A., Panzeri, L., Rondini, P., Poggiani Keller, R., Martini, M., 2020. Luminescence dating of rock surface. The case of monoliths from the megalithic sanctuary of Ossimo-Pat (Valle Camonica, Italy). *Applied Sciences* 10, 7403, <https://www.mdpi.com/2076-3417/10/21/7403>

- tephra (and volcanic related)

O'Gorman, K., Tanner, D., Sontag-González, M., Li, B., Brink, F., Jones, B.G., Dosseto, A., Jatmiko, Roberts, R.G., Jacobs, Z., 2021. Composite grains from volcanic terranes: Internal dose rates of supposed 'potassium-rich' feldspar grains used for optical dating at Liang Bua, Indonesia. *Quaternary Geochronology* 64, 101182, <http://doi.org/10.1016/j.quageo.2021.101182>

- thermochronology

Fang, F., Grün, R., 2020. ESR thermochronometry of Al and Ti centres in quartz: A case study of the Fergusons Hill-1 borehole from the Otway Basin, Australia. *Radiation Measurements* 139, 106447, <http://doi.org/10.1016/j.radmeas.2020.106447>

Archaeology applications

Aidona, E., Spassov, S., Kondopoulou, D., Polymeris, G.S., Raptis, K., Tsanana, A., 2021. Archaeomagnetism and Luminescence on Medieval kilns in Thessaloniki and Chalkidiki (N. Greece): Implications for geomagnetic field variations during the last two millennia. *Physics of the Earth and Planetary Interiors* 316, 106709, <http://doi.org/10.1016/j.pepi.2021.106709>

Álvarez-Alonso, D., Jordá Pardo, J.F., Carral, P., Flor-Blanco, G., Flor, G., Iriarte-Chiapusso, M.-J., Kehl, M., Klasen, N., Maestro, A., Rodríguez Asensio, A., Weniger, G.-C., 2020. At the edge of the Cantabrian sea. New data on the Pleistocene and Holocene archaeological open-air site of Bañugues (Gozón, Asturias, Spain): Palaeogeography, geoarchaeology and geochronology. *Quaternary International* 566-567, 284-302, <http://doi.org/10.1016/j.quaint.2020.04.025>

Araujo, A.G.d.M., Moreno de Sousa, J.C., Correa, L.C., Feathers, J.K., Okumura, M., 2021. The rise and fall of Alice Boer: A reassessment of a purported Pre-Clovis site. *PaleoAmerica* 7, 99-113, <http://doi.org/10.1080/20555563.2021.1894379>

Bahain, J.-J., Voinchet, P., Vietti, A., Shao, Q., Tombret, O., Pereira, A., Nomade, S., Falguères, C., 2021. ESR/U-series and ESR dating of several Middle Pleistocene Italian sites: Comparison with ⁴⁰Ar/³⁹Ar chronology. *Quaternary Geochronology* 63, 101151, <http://doi.org/10.1016/j.quageo.2021.101151>

Balzeau, A., Turq, A., Talamo, S., Daujeard, C., Guérin, G., Welker, F., Crevecoeur, I., Fewlass, H., Hublin, J.-J., Lahaye, C., Maureille, B., Meyer, M., Schwab, C., Gómez-Olivencia, A., 2020. Pluridisciplinary evidence for burial for the La Ferrassie 8 Neandertal child. *Scientific Reports* 10, 21230, <http://doi.org/10.1038/s41598-020-77611-z>

Barry, L., Graham, I.T., Mooney, S.D., Toms, P.S., Wood, J.C., Williams, A.N., 2021. Tracking an exotic raw material: Aboriginal movement through the Blue Mountains, Sydney, NSW during the Terminal Pleistocene. *Australian Archaeology* 87, 63-74, <http://doi.org/10.1080/03122417.2020.1823086>

Birin, R.-A., Schoeman, M.H., Evans, M., 2021. The construction and habitation of one of the earliest homesteads at Komati Gorge Village 1, Bokoni, South Africa. *Journal of Archaeological Science: Reports* 38, 103020, <http://doi.org/10.1016/j.jasrep.2021.103020>

Chambrade, M.L., Gondet, S., Laisney, D., Mehrabani, M., Mohammadkhani, K., Zareh-Kordshouli, F., 2020. The canal system of Ju-i Dokhtar: new insight into water management in the eastern part of the Pasargadae plain (Fars, Iran). *Water History* 12, 449-476, <http://doi.org/10.1007/s12685-020-00271-3>

Chevrier, B., Lespez, L., Lebrun, B., Garnier, A., Tribolo, C., Rasse, M., Guérin, G., Mercier, N., Camara, A., Ndiaye, M., Huysecom, E., 2020. New data on settlement and environment at the Pleistocene/Holocene boundary in Sudano-Sahelian West Africa: Interdisciplinary investigation at Fatandi V, Eastern Senegal. *PLOS ONE* 15, e0243129, <http://doi.org/10.1371/journal.pone.0243129>

- Dai, J., Cai, X., Jin, J., Ge, W., Huang, Y., Wu, W., Xia, T., Li, F., Zuo, X., 2021. Earliest arrival of millet in the South China coast dating back to 5,500 years ago. *Journal of Archaeological Science* 129, 105356, <http://doi.org/10.1016/j.jas.2021.105356>
- David, B., Arnold, L.J., Delannoy, J.-J., Fresløv, J., Urwin, C., Petchey, F., McDowell, M.C., Mullett, R., Mialanes, J., Wood, R., Crouch, J., Berthet, J., Wong, V.N.L., Green, H., Hellstrom, J., 2021. Late survival of megafauna refuted for Cloggs Cave, SE Australia: Implications for the Australian Late Pleistocene megafauna extinction debate. *Quaternary Science Reviews* 253, 106781, <http://doi.org/10.1016/j.quascirev.2020.106781>
- Domínguez-Solera, S.D., Moreno, D., Pérez-Garrido, C., 2020. A new complete sequence from Lower to Middle Paleolithic: El Provencio Complex (Cuenca, Spain). *Quaternary International* 566-567, 39-56, <http://doi.org/10.1016/j.quaint.2020.04.053>
- Douze, K., Lespez, L., Rasse, M., Tribolo, C., Garnier, A., Lebrun, B., Mercier, N., Ndiaye, M., Chevrier, B., Huysecom, E., 2021. A West African Middle Stone Age site dated to the beginning of MIS 5: Archaeology, chronology, and paleoenvironment of the Ravin Blanc I (eastern Senegal). *Journal of Human Evolution* 154, 102952, <http://doi.org/10.1016/j.jhevol.2021.102952>
- Friesem, D.E., Malinsky-Buller, A., Ekshtain, R., Gur-Arieh, S., Vaks, A., Mercier, N., Richard, M., Guérin, G., Valladas, H., Auger, F., Hovers, E., 2019. New Data from Shovakh Cave and Its Implications for Reconstructing Middle Paleolithic Settlement Patterns in the Amud Drainage, Israel. *Journal of Paleolithic Archaeology* 2, 298-337, <http://doi.org/10.1007/s41982-019-00028-2>
- Galli, A., Panzeri, L., Rondini, P., Poggiani Keller, R., Martini, M., 2020a. Luminescence dating of rock surface. The case of monoliths from the megalithic sanctuary of Ossimo-Pat (Valle Camonica, Italy). *Applied Sciences* 10, 7403, <https://www.mdpi.com/2076-3417/10/21/7403>
- Galli, A., Sibilia, E., Martini, M., 2020b. Ceramic chronology by luminescence dating: how and when it is possible to date ceramic artefacts. *Archaeological and Anthropological Sciences* 12, 190, <http://doi.org/10.1007/s12520-020-01140-z>
- Gueli, A.M., Garro, V., Palio, O., Pasquale, S., Politi, G., Stella, G., Turco, M., 2018. TL and OSL cross-dating for Valcorrente site in Belpasso (Catania, Italy). *The European Physical Journal Plus* 133, 542, <http://doi.org/10.1140/epjp/i2018-12364-7>
- Händel, M., Simon, U., Maier, A., Brandl, M., Groza-Săcaci, S.M., Timar-Gabor, A., Einwögerer, T., 2021. Kammern-Grubgraben revisited - First results from renewed investigations at a well-known LGM site in east Austria. *Quaternary International* 587-588, 137-157, <http://doi.org/10.1016/j.quaint.2020.06.012>
- Heydari, M., Guérin, G., Zeidi, M., Conard, N.J., 2021. Bayesian luminescence dating at Ghār-e Boof, Iran, provides a new chronology for Middle and Upper Paleolithic in the southern Zagros. *Journal of Human Evolution* 151, 102926, <http://doi.org/10.1016/j.jhevol.2020.102926>
- Hoffecker, J.F., Holliday, V.T., Nehoroshev, P., Vishnyatsky, L., Otcherednoy, A., Salnaya, N., Goldberg, P., Southon, J., Lehman, S.J., Cappa, P.J., Giaccio, B., Forman, S.L., Quade, J., 2019. The Dating of a Middle Paleolithic Blade Industry in Southern Russia and Its Relationship to the Initial Upper Paleolithic. *Journal of Paleolithic Archaeology* 2, 381-417, <http://doi.org/10.1007/s41982-019-00032-6>
- Hu, Y., Ruan, Q., Liu, J., Marwick, B., Li, B., 2020. Luminescence chronology and lithic technology of Tianhuadong Cave, an early Upper Pleistocene Paleolithic site in southwest China. *Quaternary Research* 94, 121-136, <http://doi.org/10.1017/qua.2019.67>
- Karkanas, P., Marean, C., Bar-Matthews, M., Jacobs, Z., Fisher, E., Braun, K., 2021. Cave life histories of non-anthropogenic sediments help us understand associated archaeological contexts. *Quaternary Research* 99, 270-289, <http://doi.org/10.1017/qua.2020.72>
- Li, K., Qin, X., Xu, B., Zhou, L., Jia, H., Mu, G., Wu, Y., Wei, D., Tian, X., Shao, H., Li, W., Song, H., Liu, J., Jiao, Y., 2021. Palaeofloods at ancient Loulan, northwest China: Geoarchaeological perspectives on burial practices. *Quaternary International* 577, 131-138, <http://doi.org/10.1016/j.quaint.2020.12.027>
- Liritzis, I., 2021. Kastrouli fortified settlement (Desfina, Phokis, Greece): A chronicle of research. *Scientific Culture* 7, 17-32, <https://sci-cult.com/kastrouli-fortified-settlement-desfina-phokis-greece-a-chronicle-of-research/>
- Martinón-Torres, M., d'Errico, F., Santos, E., Álvaro Gallo, A., Amano, N., Archer, W., Armitage, S.J., Arsuaga, J.L., Bermúdez de Castro, J.M., Blinkhorn, J., Crowther, A., Douka, K., Dubernet, S., Faulkner, P., Fernández-Colón, P., Kourampas, N., González García, J., Larreina, D., Le Bourdonnec, F.-X., MacLeod, G., Martín-Francés, L., Massilani, D., Mercader, J., Miller, J.M., Ndiema, E., Notario, B., Pitarch Martí, A., Prendergast, M.E., Queffelec, A., Rigaud, S., Roberts, P., Shoaee, M.J., Shipton, C., Simpson, I., Boivin, N., Petraglia, M.D., 2021. Earliest known human burial in Africa. *Nature* 593, 95-100, <http://doi.org/10.1038/s41586-021-03457-8>

- Masojeć, M., Kim, J.Y., Krupa-Kurzynowska, J., Sohn, Y.K., Ehlert, M., Michalec, G., Cendrowska, M., Andrieux, E., Armitage, S.J., Szmit, M., Dreczko, E., Kim, J.C., Kim, J.S., Lee, G.-S., Moska, P., Jadain, M.A., 2021. The oldest *Homo erectus* buried lithic horizon from the Eastern Saharan Africa. EDAR 7 - an Acheulean assemblage with Kombewa method from the Eastern Desert, Sudan. *PLOS ONE* 16, e0248279, <http://doi.org/10.1371/journal.pone.0248279>
- Peng, W., Huang, X., Storozum, M.J., Fan, Y., Zhang, H., 2021. An updated chronology and paleoenvironmental background for the Paleolithic Loufangzi site, North China. *Journal of Human Evolution* 152, 102948, <http://doi.org/10.1016/j.jhevol.2020.102948>
- Pop, E., Reidsma, F.H., Reimann, T., Sier, M.J., Arps, C.E.S., Gaudzinski-Windheuser, S., Roebroeks, W., 2021. Identifying heated rocks through feldspar luminescence analysis (pIRIR290) and a critical evaluation of macroscopic assessment. *Journal of Paleolithic Archaeology* 4, 13, <http://doi.org/10.1007/s41982-021-00094-5>
- Roos, C.I., Rittenour, T.M., Swetnam, T.W., Loehman, R.A., Hollenback, K.L., Liebmann, M.J., Rosenstein, D.D., 2020. Fire suppression impacts on fuels and fire intensity in the western U.S.: Insights from archaeological luminescence dating in northern New Mexico. *Fire* 3, 32, <http://doi.org/10.3390/fire3030032>
- Ruiz, M.N., Benito-Calvo, A., Alonso-Alcalde, R., Alonso, P., Fuente, H.d.l., Santamaría, M., Santamaría, C., Álvarez-Vena, A., Arnold, L.J., Iriarte-Chiapusso, M.J., Demuro, M., Lozano, M., Ortiz, J.E., Torres, T., 2021. Late Neanderthal subsistence strategies and cultural traditions in the northern Iberia Peninsula: Insights from Prado Vargas, Burgos, Spain. *Quaternary Science Reviews* 254, 106795, <http://doi.org/10.1016/j.quascirev.2021.106795>
- Scerri, E.M.L., Frouin, M., Breeze, P.S., Armitage, S.J., Candy, I., Groucutt, H.S., Drake, N., Parton, A., White, T.S., Alsharekh, A.M., Petraglia, M.D., 2021. The expansion of Acheulean hominins into the Nefud Desert of Arabia. *Scientific Reports* 11, 10111, <http://doi.org/10.1038/s41598-021-89489-6>
- Stavi, I., Ragolsky, G., Haiman, M., Porat, N., 2021. Ancient to recent-past runoff harvesting agriculture in the hyper-arid Arava Valley: OSL dating and insights. *The Holocene* 31, 1047-1054, <http://doi.org/10.1177/0959683621994641>
- Stephens, M., Roberts, R., Lian, O., 2016. Optical dating of sediments from the West Mouth, in: Barker, G., Farr, L. (Eds.), *Archaeological Investigations in the Niah Caves, Sarawak*. McDonald Institute for Archaeological Research, Cambridge, pp. 235-242, <https://www.arch.cam.ac.uk/mcdonald-institute-monographs/2016#NiahCaves>
- Su, K., Zhu, C., Sun, B., Jin, G., 2020. A chronology for moat construction and sedimentation at Chengziya – A late Neolithic urban settlement in Eastern China. *Journal of Archaeological Science: Reports* 29, 102046, <http://doi.org/10.1016/j.jasrep.2019.102046>
- Thompson, J.C., Wright, D.K., Ivory, S.J., Choi, J.-H., Nightingale, S., Mackay, A., Schilt, F., Otárola-Castillo, E., Mercader, J., Forman, S.L., Pietsch, T., Cohen, A.S., Arrowsmith, J.R., Welling, M., Davis, J., Schiery, B., Kaliba, P., Malijani, O., Blome, M.W., O'Driscoll, C.A., Mentzer, S.M., Miller, C., Heo, S., Choi, J., Tembo, J., Mapemba, F., Simengwa, D., Gomani-Chindebvu, E., 2021. Early human impacts and ecosystem reorganization in southern-central Africa. *Science Advances* 7, eabf9776, <http://doi.org/10.1126/sciadv.abf9776>
- Tucci, M., Krahn, K.J., Richter, D., van Kolfschoten, T., Álvarez, B.R., Verheijen, I., Serangeli, J., Lehmann, J., Degering, D., Schwalb, A., Urban, B., 2021. Evidence for the age and timing of environmental change associated with a Lower Palaeolithic site within the Middle Pleistocene Reinsdorf sequence of the Schöningen coal mine, Germany. *Palaeogeography, Palaeoclimatology, Palaeoecology* 569, 110309, <http://doi.org/10.1016/j.palaeo.2021.110309>
- Turner, S., Kinnaird, T., Varinlioglu, G., Şerifoğlu, T.E., Koparal, E., Demirciler, V., Athanasoulis, D., Ødegård, K., Crow, J., Jackson, M., Bolòs, J., Sánchez-Pardo, J.C., Carrer, F., Sanderson, D., Turner, A., 2021. Agricultural terraces in the Mediterranean: medieval intensification revealed by OSL profiling and dating. *Antiquity* 95, 773-790, <http://doi.org/10.15184/aqy.2020.187>
- Vichaidid, T., Danworaphong, S., 2021. Dating the historical old city walls of Songkhla Thailand using thermoluminescence technique. *Heliyon* 7, e06166, <http://doi.org/10.1016/j.heliyon.2021.e06166>
- Watson, S., Low, M., Phillips, N., O'Driscoll, C., Shaw, M., Ames, C., Jacobs, Z., Mackay, A., 2020. Robberg material procurement and transport in the doring river catchment: Evidence from the open-air locality of Uitspankraal 9, Western Cape, South Africa. *Journal of African Archaeology* 18, 209-228, <http://doi.org/10.1163/21915784-20200013>
- Xiaoqi, G., Chengqiu, L., Xuefeng, S., Dengke, L., Ying, L., 2021. Luminescence dating of the Huoshiwa and Houshanpo Paleolithic sites in Hanjiang River Valley, Central China. *Quaternary International* 586, 133-144, <http://doi.org/10.1016/j.quaint.2021.01.019>

Zilhão, J., Angelucci, D.E., Arnold, L.J., Demuro, M., Hoffmann, D.L., Pike, A.W.G., 2021. A revised, Last Interglacial chronology for the Middle Palaeolithic sequence of Gruta da Oliveira (Almonda karst system, Torres Novas, Portugal). *Quaternary Science Reviews* 258, 106885, <http://doi.org/10.1016/j.quascirev.2021.106885>

Various ESR applications

- Bahain, J.-J., Voinchet, P., Vietti, A., Shao, Q., Tombret, O., Pereira, A., Nomade, S., Falguères, C., 2021. ESR/U-series and ESR dating of several Middle Pleistocene Italian sites: Comparison with $^{40}\text{Ar}/^{39}\text{Ar}$ chronology. *Quaternary Geochronology* 63, 101151, <http://doi.org/10.1016/j.quageo.2021.101151>
- Bartz, M., Arnold, L.J., Spooner, N.A., Demuro, M., Campaña, I., Rixhon, G., Brückner, H., Duval, M., 2019. First experimental evaluation of the alpha efficiency in coarse-grained quartz for ESR dating purposes: implications for dose rate evaluation. *Scientific Reports* 9, 19769, <http://doi.org/10.1038/s41598-019-54688-9>
- Benzid, K., Timar-Gabor, A., 2021. On the dose dependence prior and after stimulation with visible light of E' and Al-hole centres in sedimentary quartz: Correlation and mechanisms. *Radiation Measurements* 141, 106522, <http://doi.org/10.1016/j.radmeas.2021.106522>
- Benzid, K., Timar Gabor, A., 2020. The compensation effect (Meyer–Neldel rule) on $[\text{AlO}_4/\text{h}^+]^0$ and $[\text{TiO}_4/\text{M}^+]^0$ paramagnetic centers in irradiated sedimentary quartz. *AIP Advances* 10, 075114, <http://doi.org/10.1063/5.0005161>
- Cortez, B., 2021. Dating of Sediments by physics methods Electron Paramagnetic Resonance (EPR) in the region of Iguape – Cananéia, Brazil. *Brazilian Journal of Radiation Sciences* 9, 1-13, <http://doi.org/10.15392/bjrs.v9i1A.1364>
- Domínguez-Solera, S.D., Moreno, D., Pérez-Garrido, C., 2020. A new complete sequence from Lower to Middle Paleolithic: El Provencio Complex (Cuenca, Spain). *Quaternary International* 566-567, 39-56, <http://doi.org/10.1016/j.quaint.2020.04.053>
- Fang, F., Grün, R., 2020. ESR thermochronometry of Al and Ti centres in quartz: A case study of the Fergusons Hill-1 borehole from the Otway Basin, Australia. *Radiation Measurements* 139, 106447, <http://doi.org/10.1016/j.radmeas.2020.106447>
- Guzmán, O., Díaz, M., Campos, C., González, A., Vassallo, R., Aranda, N., Conicelli, B., González-Laprea, J., 2021. First ESR dating of quaternary sediments in Mérida Andes, Western Venezuela. *Journal of South American Earth Sciences* 106, 103089, <http://doi.org/10.1016/j.jsames.2020.103089>
- Li, J., Yuan, S., Liu, Y., Liu, X., Bai, X., Jiang, J., Li, Y., Zhao, Z., 2019. Tectonic Uplift of the Yili Basin during the Last Stage of the Late Pleistocene: Evidence from ESR and OSL Dating of Sediments in the Huocheng Area, Xinjiang. *Acta Geologica Sinica - English Edition* 93, 1219-1227, <http://doi.org/10.1111/1755-6724.14355>
- Orhan, H., Delikan, A., Demir, A., Kapan, S., Olgun, K., Özmen, A., Sayın, Ü., Ekici, G., Aydın, H., Engin, B., Tapramaz, R., 2021. Late Quaternary paleoclimatic and paleoenvironmental changes in the Konya Closed Basin (Konya, Turkey) recorded by geochemical proxies from lacustrine sediments. *Arabian Journal of Geosciences* 14, 766, <http://doi.org/10.1007/s12517-021-07030-5>
- Shukla, A.K., 2021. *ESR Spectroscopy for Life Science Applications: An Introduction*. Springer, <http://doi.org/10.1007/978-3-030-64198-6>
- Toyoda, S., Murahashi, M., Natsuhori, M., Ito, S., Ivannikov, A., Todaka, A., 2019. Retrospective ESR reconstruction of cattle tooth enamel doses from the radioactive nuclei released by the accident of Fukushima Dai-Ichi atomic power plants. *Radiation Protection Dosimetry* 186, 48-53, <http://doi.org/10.1093/rpd/ncz037>
- Wang, K., Tada, R., Zheng, H., Irino, T., Zhou, B., Saito, K., 2020. Provenance changes in fine detrital quartz in the inner shelf sediments of the East China Sea associated with shifts in the East Asian summer monsoon front during the last 6 kyrs. *Progress in Earth and Planetary Science* 7, 5, <http://doi.org/10.1186/s40645-019-0319-5>
- Wu, P., Xie, Y., Chi, Y., Kang, C., Sun, L., Wei, Z., Zhang, M., Zhang, Y., 2021. Loess accumulation in Harbin with implications for late Quaternary aridification in the Songnen Plain, Northeast China. *Palaeogeography, Palaeoclimatology, Palaeoecology* 570, 110365, <http://doi.org/10.1016/j.palaeo.2021.110365>

Basic research

- Baly, L., Quesada, I., Murray, A.S., Martin, G., Espen, P., Arteché, R., Jain, M., 2021. Modeling the charge deposition in quartz grains during natural irradiation and its influence on the optically stimulated luminescence signal. *Radiation Measurements* 142, 106564, <http://doi.org/10.1016/j.radmeas.2021.106564>
- Bartyik, T., Magyar, G., Filyó, D., Tóth, O., Blanka-Végyi, V., Kiss, T., Marković, S., Persoiu, I., Gavrilov, M., Mezósi, G., Sipos, G., 2021. Spatial differences in the luminescence sensitivity of quartz extracted from Carpathian Basin fluvial sediments. *Quaternary Geochronology* 64, 101166, <http://doi.org/10.1016/j.quageo.2021.101166>
- Bartz, M., Arnold, L.J., Spooner, N.A., Demuro, M., Campaña, I., Rixhon, G., Brückner, H., Duval, M., 2019. First experimental evaluation of the alpha efficiency in coarse-grained quartz for ESR dating purposes: implications for dose rate evaluation. *Scientific Reports* 9, 19769, <http://doi.org/10.1038/s41598-019-54688-9>
- Benzid, K., Timar-Gabor, A., 2021. On the dose dependence prior and after stimulation with visible light of E' and Al-hole centres in sedimentary quartz: Correlation and mechanisms. *Radiation Measurements* 141, 106522, <http://doi.org/10.1016/j.radmeas.2021.106522>
- Benzid, K., Timar Gabor, A., 2020. The compensation effect (Meyer–Neldel rule) on $[AlO_4/h^+]^0$ and $[TiO_4/M^+]^0$ paramagnetic centers in irradiated sedimentary quartz. *AIP Advances* 10, 075114, <http://doi.org/10.1063/5.0005161>
- Chen, R., Lawless, J.L., Pagonis, V., 2021. Thermoluminescence due to simultaneous recombination of two electrons into two-hole centers. *Radiation Measurements* 141, 106521, <http://doi.org/10.1016/j.radmeas.2021.106521>
- Dawam, R.R., Masok, F.B., Fierkwap, S.B., 2021. Thermoluminescence of secondary peak on synthetic quartz: Influence of annealing time on kinetic parameters and some dosimetric features. *Journal of Luminescence* 233, 117918, <http://doi.org/10.1016/j.jlumin.2021.117918>
- Elkadi, J., King, G.E., Lehmann, B., Herman, F., 2021. Reducing variability in OSL rock surface dating profiles. *Quaternary Geochronology* 64, 101169, <http://doi.org/10.1016/j.quageo.2021.101169>
- Kumar, R., Kook, M., Jain, M., 2021. Sediment dating using Infrared Photoluminescence. *Quaternary Geochronology* 62, 101147, <http://doi.org/10.1016/j.quageo.2020.101147>
- Li, Z., Mou, X., Fan, Y., Zhang, Q., Yang, G., Zhao, H., 2020. Establishing a common standardised growth curve for single-aliquot OSL dating of quartz from sediments in the Jilantai area of North China. *Geochronometria* 47, 71-92, <http://doi.org/10.2478/geochr-2020-0017>
- Mammadov, S., Samedov, O., Gurbanov, M., Bayramov, M., Abishov, A., Ahadova, A., 2020. Thermoluminescence properties of irradiated quartz and feldspar at different dose rates. *Journal of Radiation Researches* 7, 70-75, [http://irp.science.az/dw.php?l=/uploads/pdf/11\) journal of radiation researches, vol.7, n 2, 2020 70-75.pdf](http://irp.science.az/dw.php?l=/uploads/pdf/11) journal of radiation researches, vol.7, n 2, 2020 70-75.pdf)
- Mineli, T.D., Sawakuchi, A.O., Guralnik, B., Lambert, R., Jain, M., Pupim, F.N., Rio, I.d., Guedes, C.C.F., Nogueira, L., 2021. Variation of luminescence sensitivity, characteristic dose and trap parameters of quartz from rocks and sediments. *Radiation Measurements* 144, 106583, <http://doi.org/10.1016/j.radmeas.2021.106583>
- Mittelstraß, D., Kreuzer, S., 2021. Spatially resolved infrared radiofluorescence: single-grain K-feldspar dating using CCD imaging. *Geochronology* 3, 299-319, <http://doi.org/10.5194/gchron-3-299-2021>
- Ngoc, T., Van Tuyen, H., Thi, L.A., Hung, L.X., Ca, N.X., Thanh, L.D., Van Do, P., Son, N.M., Thanh, N.T., Quang, V.X., 2021. The role of sodium ions in the thermoluminescence peaks of laboratory-irradiated natural quartz. *Radiation Measurements* 141, 106539, <http://doi.org/10.1016/j.radmeas.2021.106539>
- Pagonis, V., Kitis, G., Chen, R., 2020. A new analytical equation for the dose response of dosimetric materials, based on the Lambert W function. *Journal of Luminescence* 225, 117333, <http://doi.org/10.1016/j.jlumin.2020.117333>
- Peng, J., Wang, X., Adamiec, G., Pagonis, V., Choi, J.-H., 2021. Modelling the dependence of equivalent dose determined from a dose recovery test on preheating temperature: The intervention of shallow electron traps. *Radiation Measurements* 142, 106566, <http://doi.org/10.1016/j.radmeas.2021.106566>
- Richter, D., Woda, C., Dornich, K., 2020. A new quartz for g-transfer calibration of radiation sources. *Geochronometria* 47, 23-34, <http://doi.org/10.2478/geochr-2020-0020>
- Riedesel, S., Bell, A.M.T., Duller, G.A.T., Finch, A.A., Jain, M., King, G.E., Pearce, N.J., Roberts, H.M., 2021. Exploring sources of variation in thermoluminescence emissions and anomalous fading in alkali feldspars. *Radiation Measurements* 141, 106541, <http://doi.org/10.1016/j.radmeas.2021.106541>

- Stalder, R., 2021. OH point defects in quartz – a review. *European Journal of Mineralogy* 33, 145-163, <http://doi.org/10.5194/ejm-33-145-2021>
- Wang, K., Tada, R., Zheng, H., Irino, T., Zhou, B., Saito, K., 2020. Provenance changes in fine detrital quartz in the inner shelf sediments of the East China Sea associated with shifts in the East Asian summer monsoon front during the last 6 kyrs. *Progress in Earth and Planetary Science* 7, 5, <http://doi.org/10.1186/s40645-019-0319-5>
- Wang, X., Peng, J., Adamiec, G., 2021. Extending the age limit of quartz OSL dating of Chinese loess using a new multiple-aliquot regenerative-dose (MAR) protocol with carefully selected preheat conditions. *Quaternary Geochronology* 62, 101144, <http://doi.org/10.1016/j.quageo.2020.101144>

Dose rate issues

- Bartz, M., Arnold, L.J., Spooner, N.A., Demuro, M., Campaña, I., Rixhon, G., Brückner, H., Duval, M., 2019. First experimental evaluation of the alpha efficiency in coarse-grained quartz for ESR dating purposes: implications for dose rate evaluation. *Scientific Reports* 9, 19769, <http://doi.org/10.1038/s41598-019-54688-9>
- Heydari, M., Guérin, G., Zeidi, M., Conard, N.J., 2021. Bayesian luminescence dating at Ghār-e Boof, Iran, provides a new chronology for Middle and Upper Paleolithic in the southern Zagros. *Journal of Human Evolution* 151, 102926, <http://doi.org/10.1016/j.jhevol.2020.102926>
- O'Gorman, K., Brink, F., Tanner, D., Li, B., Jacobs, Z., 2021. Calibration of a QEM-EDS system for rapid determination of potassium concentrations of feldspar grains used in optical dating. *Quaternary Geochronology* 61, 101123, <http://doi.org/10.1016/j.quageo.2020.101123>
- O'Gorman, K., Tanner, D., Sontag-González, M., Li, B., Brink, F., Jones, B.G., Dosseto, A., Jatmiko, Roberts, R.G., Jacobs, Z., 2021. Composite grains from volcanic terranes: Internal dose rates of supposed 'potassium-rich' feldspar grains used for optical dating at Liang Bua, Indonesia. *Quaternary Geochronology* 64, 101182, <http://doi.org/10.1016/j.quageo.2021.101182>

Dosimetry

- Asfora, V.K., Antonio, P.L., Gonçalves, J.A.C., Bueno, C.C., de Barros, V.S.M., Oliveira, C.N.P., Caldas, L.V.E., Khoury, H.J., 2021. Evaluation of TL and OSL responses of CaF₂:Tm for electron beam processing dosimetry. *Radiation Measurements* 140, 106512, <http://doi.org/10.1016/j.radmeas.2020.106512>
- Chrisanthakopoulos, A., Santos, A.M.C., 2021. The intrinsic x-ray energy dependence of beryllium oxide (BeO) ceramic dosimeters. *Radiation Measurements* 141, 106537, <http://doi.org/10.1016/j.radmeas.2021.106537>
- Discher, M., Woda, C., Ekendahl, D., Rojas-Palma, C., Steinhäusler, F., 2021. Evaluation of physical retrospective dosimetry methods in a realistic accident scenario: Results of a field test. *Radiation Measurements* 142, 106544, <http://doi.org/10.1016/j.radmeas.2021.106544>
- Geranmayeh, S., Şahiner, E., Aşlar, E., Polymeris, G.S., Meriç, N., 2021. Comparison of stimulated luminescence properties of various porcelain-based items from Turkey towards prevalent features for retrospective dosimetry. *Nuclear Instruments and Methods in Physics Research Section B: Beam Interactions with Materials and Atoms* 499, 89-99, <http://doi.org/10.1016/j.nimb.2021.05.007>
- Iurlaro, G., Baranowska, Z., Campani, L., Bjelac, O.C., Ferrari, P., Knežević, Ž., Majer, M., Mariotti, F., Morelli, B., Neumaier, S., Nodilo, M., Sperandio, L., Vittoria, F.A., Wołoszczuk, K., Živanovic, M., 2021. Study on the uncertainty of passive area dosimetry systems for environmental radiation monitoring in the framework of the EMPIR "Preparedness" project. *Radiation Measurements* 142, 106543, <http://doi.org/10.1016/j.radmeas.2021.106543>
- Nikiforov, S.V., Tsepilov, M.V., Ananchenko, D.V., Ishchenko, A.V., Gerasimov, M.F., 2020. Luminescent and dosimetric properties of transition phases of nanostructured aluminum oxide. *Radiation Measurements* 139, 106466, <http://doi.org/10.1016/j.radmeas.2020.106466>
- Polymeris, G.S., Çoskun, S., Tsoutsoumanos, E., Konstantinidis, P., Aşlar, E., Şahiner, E., Meriç, N., Kitis, G., 2021. Dose response features of quenched and reconstructed, TL and deconvolved OSL signals in BeO. *Results in Physics* 25, 104222, <http://doi.org/10.1016/j.rinp.2021.104222>
- Sholom, S., McKeever, S.W.S., 2021. OSL with chips from US credit cards. *Radiation Measurements* 141, 106536, <http://doi.org/10.1016/j.radmeas.2021.106536>

- Stella, G., Cavalli, N., Marino, C., Mazzaglia, S., Gueli, A.M., 2019. Dosimetry from OSL and Residual TL with TLD 400. *Journal of Instrumentation* 14, P12014-P12014, <http://doi.org/10.1088/1748-0221/14/12/p12014>
- Toyoda, S., Murahashi, M., Natsuhori, M., Ito, S., Ivannikov, A., Todaka, A., 2019. Retrospective ESR reconstruction of cattle tooth enamel doses from the radioactive nuclei released by the accident of Fukushima Dai-Ichi atomic power plants. *Radiation Protection Dosimetry* 186, 48-53, <http://doi.org/10.1093/rpd/ncz037>
- Ulanowski, A., Hiller, M., Woda, C., 2021. Absorbed doses in bricks and TL-dosimeters due to anthropogenic and natural environmental radiation sources. *Radiation Measurements* 140, 106458, <http://doi.org/10.1016/j.radmeas.2020.106458>
- Van Hoey, O., Römken, D., Eakins, J., Kouroukla, E., Discher, M., Vanhavere, F., 2021. Uncertainty evaluation for organ dose assessment with optically stimulated luminescence measurements on mobile phone resistors after a radiological incident. *Radiation Measurements* 141, 106520, <http://doi.org/10.1016/j.radmeas.2021.106520>
- Yasuda, H., Discher, M., 2020. Estimation of dose and elapsed time after unrecognized high-dose radiation exposure using the continuous-wave optically stimulated luminescence from Mg₂SiO₄:Tb. *Radiation Measurements* 139, 106474, <http://doi.org/10.1016/j.radmeas.2020.106474>
- Yukihara, E.G., Kron, T., 2020. Applications of optically stimulated luminescence in medical dosimetry. *Radiation Protection Dosimetry* 192, 122-138, <http://doi.org/10.1093/rpd/ncaa213>

Instruments

- Mittelstraß, D., Kreutzer, S., 2021. Spatially resolved infrared radiofluorescence: single-grain K-feldspar dating using CCD imaging. *Geochronology* 3, 299-319, <http://doi.org/10.5194/gchron-3-299-2021>

Portable instruments

- Munyikwa, K., Kinnaird, T.C., Sanderson, D.C.W., 2021. The potential of portable luminescence readers in geomorphological investigations: a review. *Earth Surface Processes and Landforms* 46, 131-150, <http://doi.org/10.1002/esp.4975>
- Robins, L., Greenbaum, N., Yu, L., Bookman, R., Roskin, J., 2021. High-resolution portable-OSL analysis of Vegetated Linear Dune construction in the margins of the northwestern Negev dunefield (Israel) during the late Quaternary. *Aeolian Research* 50, 100680, <http://doi.org/10.1016/j.aeolia.2021.100680>
- Turner, S., Kinnaird, T., Varinlioğlu, G., Şerifoğlu, T.E., Koparal, E., Demirciler, V., Athanasoulis, D., Ødegård, K., Crow, J., Jackson, M., Bolòs, J., Sánchez-Pardo, J.C., Carrer, F., Sanderson, D., Turner, A., 2021. Agricultural terraces in the Mediterranean: medieval intensification revealed by OSL profiling and dating. *Antiquity* 95, 773-790, <http://doi.org/10.15184/aqy.2020.187>

Computer coding

- Guérin, G., Lahaye, C., Heydari, M., Autzen, M., Buylaert, J.-P., Guibert, P., Jain, M., Kreutzer, S., Lebrun, B., Murray, A.S., Thomsen, K.J., Urbanova, P., Philippe, A., 2021. Towards an improvement of optically stimulated luminescence (OSL) age uncertainties: modelling OSL ages with systematic errors, stratigraphic constraints and radiocarbon ages using the R package BayLum. *Geochronology* 3, 229-245, <http://doi.org/10.5194/gchron-3-229-2021>
- Pagonis, V., 2021. *Luminescence: Data Analysis and Modeling Using R*. Springer International Publishing, <http://doi.org/10.1007/978-3-030-67311-6>
- Pagonis, V., Schmidt, C., Kreutzer, S., 2021. Simulating feldspar luminescence phenomena using R. *Journal of Luminescence* 235, 117999, <http://doi.org/10.1016/j.jlumin.2021.117999>

- database

- Peters, K.J., Saltré, F., Friedrich, T., Jacobs, Z., Wood, R., McDowell, M., Ulm, S., Bradshaw, C.J.A., 2019. FosSahul 2.0, an updated database for the Late Quaternary fossil records of Sahul. *Scientific Data* 6, 272, <http://doi.org/10.1038/s41597-019-0267-3>

Review

- Galli, A., Sibilia, E., Martini, M., 2020. Ceramic chronology by luminescence dating: how and when it is possible to date ceramic artefacts. *Archaeological and Anthropological Sciences* 12, 190, <http://doi.org/10.1007/s12520-020-01140-z>
- Moska, P., Bluszcz, A., Poręba, G., Tudyka, K., Adamiec, G., Szymak, A., Przybyła, A., 2021. Luminescence dating procedures at the Gliwice luminescence dating laboratory. *Geochronometria* 48, 1-15, <http://doi.org/10.2478/geochr-2021-0001>
- Munyikwa, K., Kinnaird, T.C., Sanderson, D.C.W., 2021. The potential of portable luminescence readers in geomorphological investigations: a review. *Earth Surface Processes and Landforms* 46, 131-150, <http://doi.org/10.1002/esp.4975>
- Murari, M.K., Kreutzer, S., King, G., Frouin, M., Tsukamoto, S., Schmidt, C., Lauer, T., Klasen, N., Richter, D., Friedrich, J., Mercier, N., Fuchs, M., 2021. Infrared radiofluorescence (IR-RF) dating: A review. *Quaternary Geochronology* 64, 101155, <http://doi.org/10.1016/j.quageo.2021.101155>
- Pagonis, V., 2021. *Luminescence: Data Analysis and Modeling Using R*. Springer International Publishing, <http://doi.org/10.1007/978-3-030-67311-6>
- Shukla, A.K., 2021. *ESR Spectroscopy for Life Science Applications: An Introduction*. Springer, <http://doi.org/10.1007/978-3-030-64198-6>
- Stalder, R., 2021. OH point defects in quartz – a review. *European Journal of Mineralogy* 33, 145-163, <http://doi.org/10.5194/ejm-33-145-2021>
- Wallinga, J., Sevink, J., van Mourik, J.M., Reimann, T., 2019. Chapter 4 - Luminescence dating of soil archives, 18. in: Van Mourik, J.M., Van Der Meer, J.J.M. (Eds.), *Reading the Soil Archives: Unraveling the geocological code of palaeosols and sediment cores*. Elsevier, pp. 115-162, <http://doi.org/10.1016/B978-0-444-64108-3.00004-5>
- Yukihara, E.G., Kron, T., 2020. Applications of optically stimulated luminescence in medical dosimetry. *Radiation Protection Dosimetry* 192, 122-138, <http://doi.org/10.1093/rpd/ncaa213>

Conference Announcements: **LED 2021**



16th International Luminescence and Electron Spin Resonance Dating conference (LED2021)

13 to 17th September 2021

The 16th International Luminescence and Electron Spin Resonance Dating conference (LED2021) will take place online from 13 to 17th September 2021. The last conference in this series was held in Cape Town in 2017, and the next conference in the series was to be held in person in Burgos in 2020 or 2021, but due to the ongoing uncertainty regarding COVID-19 it is not possible to meet in person at this time. However, to ensure that we can retain the opportunity to come together (albeit virtually) and present our latest research, there will be an online conference this year.

Conference organisation for LED2021 is an international collaboration involving members of the standing Scientific Organising Committee with additional international representation. The aim of the conference is to provide a stimulating academic environment for presentation and discussion. The conference will cover similar themes to previous conferences in this series, and papers presented at the conference will be eligible for submission to one of the two special issues arising from the conference, one in Quaternary Geochronology, and one in Radiation Measurements.

More information can be found at : <https://led2021.wordpress.com/>

From the LED2021 International Scientific Organising Committee:

Lee Arnold, Andrzej Bluszcz, Regina DeWitt, Geoff Duller, Christophe Falguères, Mayank Jain, Gloria I. López, P Morthekai, Naomi Porat, Sumiko Tsukamoto, Liping Zhou

Conference Announcements: 2nd SHIC

To promote mutual interest in cultural and environmental issues on a global scale, the University of the Aegean, Greece and Henan University, China as part of an research & educational agreement are announcing the 2nd jointly organized conference on **Global issues of Environment & Culture**.

The Sino-Hellenic International Conference (SHIC) is a series of international conferences hosted in China and Greece alternatively. The 2nd SHIC on Environment & Culture will take place on 18-19 September 2021, at the European Cultural Center of Delphi, and a cultural event is planned for 17th Sept (if Covid-19 measures permit). Due to COVID-19 we offer online video conference presentation from your office at home.

The 2nd International Conference is one of the activities of the Project “Sino-Hellenic Academic Project” of the Research Center of Hellenic Civilization (Henan Univ, Kaifeng), the Research Center of Yellow River Civilization in Greece, and the Collaborative Innovation Center on Yellow River Civilization and Sustainable Development.

The 2nd Sino-Hellenic International Conference welcomes contribution on any topics related to the environment and cultures globally. Session topics include *Archaeology & Archaeometry* and *Cultural Geography & Geosciences*. The sessions also include luminescence related presentations.

More information can be found at : <https://shap-conference.com/>

We are looking forward to your active participation.

Respectfully

Prof. Ioannis Liritzis
University of the Aegean

and

Prof. Miao Changhong
Henan University

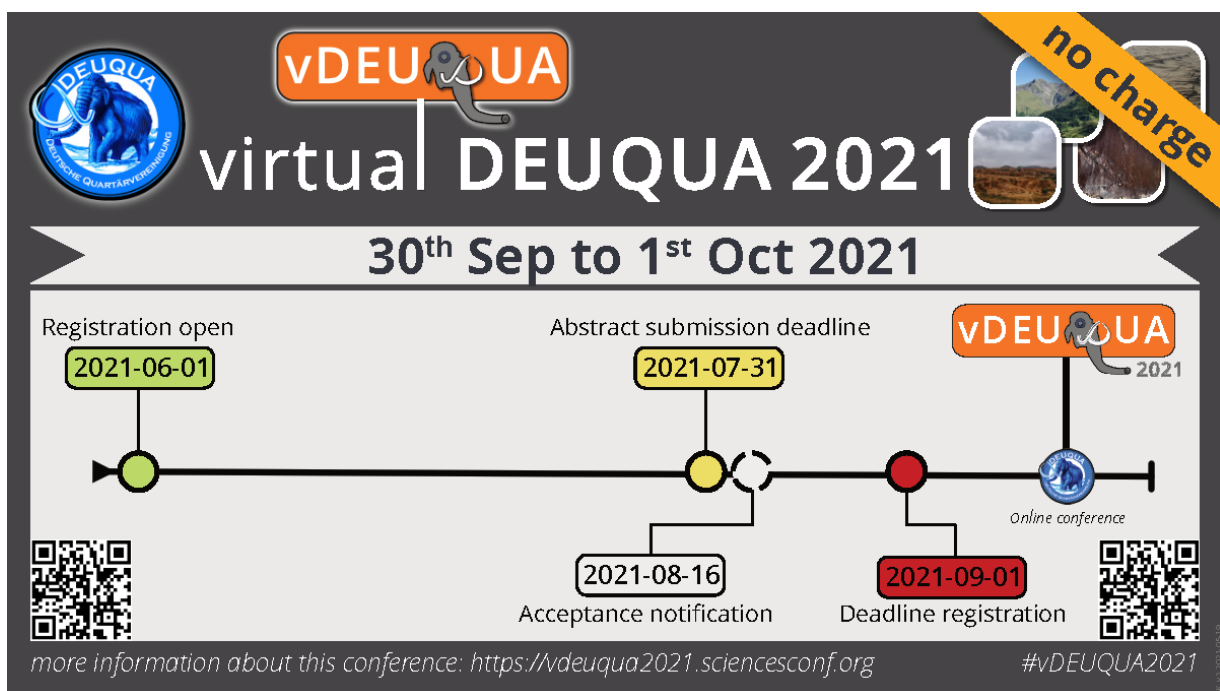
Conference Announcements: **virtual DEUQUA 2021**

We are delighted to announce that the annual meeting of the German Quaternary Association will take place from 2021-09-30 to 2021-10-01. Due to the ongoing pandemic situation with uncertain prospects for travelling, the conference will be moved into the virtual space (#vDEUQUA2021). We especially encourage young scientists to present their research and get in touch with actual issues of Quaternary research.

The programme will consist of “classical” oral presentations with subsequent discussions and short presentations to exchange views in individual chats. The preferred presentation language is English. However, naturally, contributions in German are possible. For the evening 2021-09-30, we are planning on organising a virtual get-together.

Thanks to the generous support by the DEUQUA, we happily waive the conference fees and offer this online conference free of charge.

For more information see: <https://vdeuqua2021.sciencesconf.org/>



Conference Announcements: 6th APLED

Dear Colleagues,

It is a good opportunity to discuss with you the latest update regarding the 6th Asian Pacific Luminescence and Electron Spin Resonance (APLED) conference, which is to be organised by Ankara University. As you may remember, initially the 6th APLED Conference was planned to be held in Antalya, Turkey during September 2021. Due to the COVID-19 crisis, though, it was not possible to organize the conference as planned and thus we had decided to postpone it. Unfortunately, the COVID-19 pandemic that so deeply has affected and still affects our lives and countries is not expected to end very soon, and its consequences will be present for a long time. After careful consideration by the APLED scientific committee, and in light of the ongoing Coronavirus (COVID-19) developments, we sadly made a decision to further postpone the APLED conference. Even though, the situation has not considerably improved since then, we see a realistic chance that it will be possible to organize the conference in the future. For this, we would like to give it another try and keep our promise, by inviting you to Turkey later on. We will get back to you with more information on specific dates in the coming announcements. We hope that next year conditions will be much more in favour for organizing a conference.

Attending a conference was never just about studying - it also includes social aspects such as networking, meeting friends and colleagues and understanding different cultures. These are the reasons why all of us love attending conferences.

Please take a moment to let us know if you have any questions; your feedback is important for us.

We look forward to hosting you in Anatolia, one among the few places all around the world where history dominates.

Until then, stay safe and healthy!

On behalf of the local organising committee

Prof. Dr. Niyazi MERİÇ
Dr. George S. POLYMERIS
Dr. Eren ŞAHİNER

Ancient TL

ISSN 2693-0935

Aims and Scope

Ancient TL is a journal devoted to Luminescence dating, Electron Spin Resonance (ESR) dating, and related techniques. It aims to publish papers dealing with experimental and theoretical results in this field, with a minimum of delay between submission and publication. Ancient TL also publishes a current bibliography, thesis abstracts, letters, and miscellaneous information, e.g., announcements for meetings.

Frequency

Two issues per annum in June and December

Submission of articles to Ancient TL

Ancient TL has a reviewing system in which direct dialogue is encouraged between reviewers and authors. For instructions to authors and information on how to submit to Ancient TL, please visit the website at:

<http://ancienttl.org/TOC1.htm>

Journal Enquiries

For enquiries please contact the editor:

Regina DeWitt, Department of Physics, East Carolina University, Howell Science Complex, 1000 E. 5th Street, Greenville, NC 27858, USA; Tel: +252-328-4980; Fax: +252-328-0753 (dewittr@ecu.edu)

Subscriptions to Ancient TL

Ancient TL Vol. 32 No.2 December 2014 was the last issue to be published in print. Past and current issues are available for download free of charge from the Ancient TL website:

<http://ancienttl.org/TOC4.htm>